First Observation of *CP* Violation and Measurement of Polarization in $B^+ \to \rho(770)^0 K^*(892)^+$ Decays

R. Aaij *et al.*[*]
(LHCb Collaboration)

(Received 21 August 2025; accepted 12 December 2025; published 14 January 2026)

An amplitude analysis of the $B^+ \to (\pi^+\pi^-)(K^0_S\pi^+)$ decay is performed in the mass regions $0.30 < m_{\pi^+\pi^-} < 1.10$ GeV/c^2 and $0.75 < m_{K^0_S\pi^+} < 1.20$ GeV/c^2, using pp collision data recorded with the LHCb detector corresponding to an integrated luminosity of 9 fb^{-1}. The polarization fractions and *CP* asymmetries for $B^+ \to \rho(770)^0 K^*(892)^+$ decays are measured. Violation of the *CP* symmetry in the decay $B^+ \to \rho(770)^0 K^*(892)^+$ is observed for the first time, with a significance exceeding 9 standard deviations. The *CP* asymmetry is measured to be $\mathcal{A}_{CP} = 0.507 \pm 0.062(\text{stat}) \pm 0.024(\text{syst})$ and the *CP*-averaged longitudinal polarization fraction of $f_L = 0.720 \pm 0.028(\text{stat}) \pm 0.009(\text{syst})$. The measurements help to shed light on the polarization puzzle of B mesons decaying to two vector mesons.

DOI: 10.1103/9zhl-kkwg

Decays of beauty mesons provide a rich phenomenology to study the standard model (SM) of particle physics and investigate potential new physics effects. Charmless B-meson decays into two vector mesons (V), $B \to VV$, serve as a powerful probe for the dynamics of weak and strong interactions through their angular distributions. Since $B \to VV$ decays generally proceed through transitions at both leading-order (tree-level) and higher-order (loop), they carry information about the SM flavor structure and the Cabibbo-Kobayashi-Maskawa matrix [1]. The interference between the loop and tree-level processes gives rise to the combined charge conjugation and parity (*CP*) violation, a phenomenon required to explain the matter-antimatter asymmetry of the Universe.

Every $B \to VV$ decay receives contributions from three helicity amplitudes, which, with an appropriate choice of basis, can be described by longitudinal (A_0), perpendicular ($A_\perp$), and parallel ($A_\parallel$) components encoding different orbital angular momentum configurations between the two vector mesons [2], allowing to study the spin structure of the flavor-changing interaction. These amplitudes can be distinguished by studying the angular distributions of the decay products of the two vector mesons, enabling measurements of the weak and strong phases, as well as the longitudinal polarization fraction $f_L \equiv |A_0|^2/(|A_0|^2 + |A_\perp|^2 + |A_\parallel|^2)$. While the SM predicts an almost total longitudinal polarization, $f_L \approx 1$, by a naive factorization ansatz [3], f_L is measured to span the range from around 10% to almost 100% across different $B \to VV$ decay modes [4–17]. Explanations proposed to resolve this "polarization puzzle" include enhanced contributions from weak-annihilation amplitudes [18–22], charm-loop diagrams [23,24], higher-order corrections [25,26], final-state interactions [27–30], as well as physics beyond the SM [31–36]. These contributions may also have a significant impact on predictions of *CP* asymmetries in $B \to VV$ decays [26]. To date, a coherent description of *CP* violation and polarization in $B \to VV$ decays remains challenging.

The specific class of $B \to VV$ decays with $B \to \rho K^*$ has been widely studied, where, throughout this Letter, ρ and K^* represent the $\rho(770)$ and $K^*(892)$ mesons, respectively, unless otherwise stated. The longitudinal fractions are measured to be substantially different depending on the final state, with $f_L(B^+ \to \rho^0 K^{*+}) = 0.78 \pm 0.12$ [37], $f_L(B^+ \to \rho^+ K^{*0}) = 0.48 \pm 0.08$ [5,38,39], $f_L(B^0 \to \rho^0 K^{*0}) = 0.173 \pm 0.026$ [15,38,40], and $f_L(B^0 \to \rho^- K^{*+}) = 0.38 \pm 0.13$ [40], where charge conjugation is implied throughout this Letter unless otherwise specifically stated. These observed discrepancies reflect the varying interference patterns between tree-level and loop processes [41], which would also be revealed by measuring the *CP* asymmetries. Among these decays, *CP* violation has only been established in the longitudinal component of the $B^0 \to \rho^0 K^{*0}$ decay [15]. Detailed and precise measurements of $B \to \rho K^*$ decays, compared with various predictions [2,20–22,24,25,41–46], permit more precise extractions of nonperturbative parameters through global fits [46] and help to shed light on the polarization puzzle and the dynamics of *CP* violation in these decays. They also comprise fundamental input for theoretically clean,

[*]Full author list given at the end of the Letter.

model-independent isospin sum rules that are highly sensitive to physics beyond the SM [47].

In this Letter the measurements of polarization and CP parameters in the $B^+ \to \rho^0 K^{*+}$ decay are reported. The reconstruction of the ρ^0 and K^{*+} mesons are performed in the decays $\rho^0 \to \pi^+\pi^-$ and $K^{*+} \to K^0_S\pi^+$, respectively. An amplitude analysis of the $B^+ \to (\pi^+\pi^-)(K^0_S\pi^+)$ decay is performed, using pp collision data collected with the LHCb detector at center-of-mass energies of $\sqrt{s} = 7$, 8 (Run 1 period in years 2011 and 2012) and 13 TeV (Run 2 period in years 2015–2018), corresponding to a total integrated luminosity of 9 fb^{-1}.

The LHCb detector is a single-arm forward spectrometer dedicated to the study of heavy flavor hadrons and is described in detail in Refs. [48,49]. The online event selection is performed by a trigger [50,51], which consists of a hardware stage followed by a software stage. The hardware trigger selects hadron, muon, electron, and photon candidates with high transverse momentum (p_T) based on information from the calorimeter and muon systems. The software stage, which applies a full event reconstruction, identifies a secondary vertex with a significant displacement from any primary pp interaction vertex (PV) by means of a multivariate algorithm. Simulated $B^+ \to \rho^0 K^{*+}$ decays are produced with the software described in Refs. [52–59], and are used to model the effects of the detector acceptance, resolution, and selection requirements. The simulation is subjected to the same selection requirements applied to data.

In the off-line analysis, five charged tracks identified as pions are used to build the B^+ candidate according to the decay sequence $B^+ \to \rho^0(\to \pi^+\pi^-)K^{*+}(\to K^0_S\pi^+)$, with $K^0_S \to \pi^+\pi^-$. The pions are required to be inconsistent with being produced from any PV. The K^0_S, ρ^0, K^{*+}, and B^+ candidates are required to have well-reconstructed decay vertices [49] and significant displacement from any PV. The reconstructed K^0_S mass should be consistent with its known value [38]. The masses of ρ^0 and K^{*+} candidates are required to be within the ranges $0.30 < m_{\pi^+\pi^-} < 1.10\,\mathrm{GeV}/c^2$ and $0.75 < m_{K^0_S\pi^+} < 1.20$ GeV/c^2, respectively, to contain most of the resonant contributions given their large natural widths. After applying the two mass-window requirements, candidates with the interchange of the two same-charge pions are negligible. Any B^+ candidate with mass in the range $4.90 < m_{\pi^+\pi^-K^0_S\pi^+} < 5.80$ GeV/c^2 is retained for further analysis.

The $K^0_S \to \pi^+\pi^-$ candidates are contaminated by $\Lambda \to p\pi^-$ decays, where the proton is misidentified as a pion. This background is reduced to a negligible level by vetoing K^0_S candidates with mass consistent with the known Λ mass [38], when the energy of a pion is calculated under the proton mass hypothesis. The same approach is applied to suppress decays involving intermediate charmed states. For example, the $B^+ \to \bar{D}^0(\to K^0_S\pi^+\pi^-)\pi^+$ decay is removed by vetoing candidates with $K^0_S\pi^+\pi^-$ mass near the known D^0 mass [38].

To further suppress background due to random combinations of final-state tracks, a boosted decision tree (BDT) classifier [60,61] implemented in the TMVA toolkit [62,63] is employed. The variables discriminating signal and background include the geometrical and kinematical properties of the decay. The BDT classifier is trained using simulated $B^+ \to \rho^0 K^{*+}$ decays as a proxy for the signal and data candidates in the high $\pi^+\pi^-K^0_S\pi^+$ mass region, $5.40 < m_{\pi^+\pi^-K^0_S\pi^+} < 5.80$ GeV/c^2, for the background. The requirement on the BDT response is optimized simultaneously with the particle identification of pions, by maximizing the figure of merit defined as $S/\sqrt{S+B}$. The quantities S and B are the signal and background yields estimated in the signal region chosen as ± 0.043 GeV/c^2 around the known B^+ mass of 5.279 GeV/c^2 [38], approximately 2.5 times the experimental mass resolution.

An extended unbinned maximum-likelihood fit is performed simultaneously to the $m_{\pi^+\pi^-K^0_S\pi^+}$ and $m_{\pi^-\pi^+K^0_S\pi^-}$ distributions in the range $4.90 < m_{\pi^\pm\pi^\mp K^0_S\pi^\pm} < 5.60\,\mathrm{GeV}/c^2$, as shown in Fig. 1, where the shape parameters for each component are shared for B^+ and B^- decays, with the yields allowed to differ between the two samples. The fit model consists of the combination of a Gaussian function and a Crystal Ball function [64] to describe the signal, and an exponential function for the combinatorial background. An ARGUS function [65] is used to describe partially reconstructed backgrounds, such as the $B^{0,+} \to (\pi^+\pi^-)(K^0_S\pi^+)\pi^{-,0}$ decay where the additional $\pi^{-,0}$ meson is not reconstructed. The numbers of B^+ and B^- signal candidates are determined to be 2208 ± 53 and 2333 ± 55, respectively, where the uncertainties are statistical. The subsequent amplitude analysis exploits candidates in the signal region, chosen as $5.24 < m_{\pi^\pm\pi^\mp K^0_S\pi^\pm} < 5.32\,\mathrm{GeV}/c^2$. Within this region, the fraction of B^+ (B^-) combinatorial background over the total signal and background yield of both flavors is $r_b^+ = 0.0631 \pm 0.0032$ ($r_b^- = 0.0633 \pm 0.0032$), where the uncertainties are statistical only. The charge asymmetry is not significant for either the combinatorial background or the signal. The amount of partially reconstructed background in the signal regions is negligible.

An amplitude analysis is performed to study the different contributions to the decay, thereby enabling measurements of the polarization and the CP asymmetry for each component. The kinematics of the $B^+ \to (\pi^+\pi^-)(K^0_S\pi^+)$ decay can be fully described by five independent variables, $\vec{\mathcal{O}} = (m_{\pi^+\pi^-}, m_{K^0_S\pi^+}, \cos\theta_{\pi^+\pi^-}, \cos\theta_{K^0_S\pi^+}, \phi)$, where $m_{\pi^+\pi^-}$ and $m_{K^0_S\pi^+}$ are the masses, $\theta_{\pi^+\pi^-}$ and $\theta_{K^0_S\pi^+}$ are the helicity angles, and ϕ is the angle between the $\rho^0 \to \pi^+\pi^-$ and $K^{*+} \to K^0_S\pi^+$ decay planes. The variable $\theta_{\pi^+\pi^-}$ ($\theta_{K^0_S\pi^+}$) is

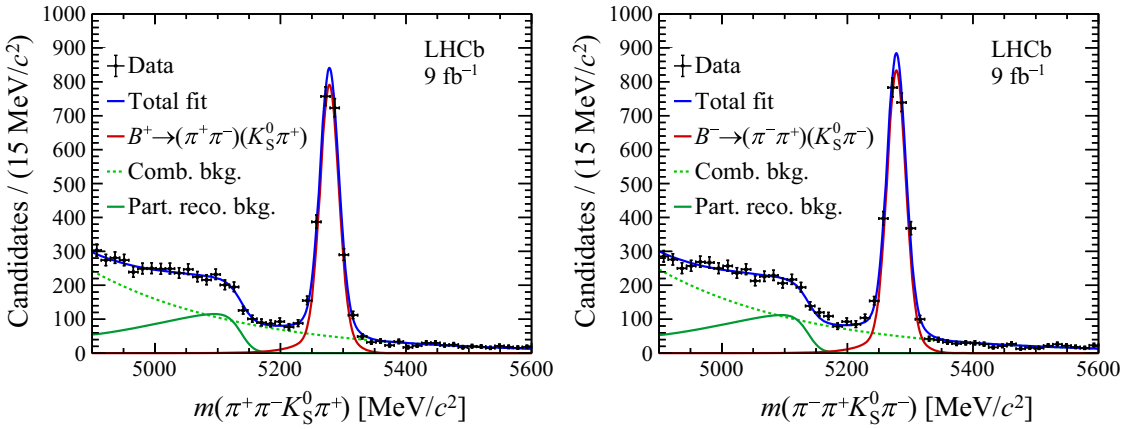

FIG. 1. Mass distributions of (left) $B^+ \to (\pi^+\pi^-)(K^0_S\pi^+)$ and (right) $B^- \to (\pi^-\pi^+)(K^0_S\pi^-)$ candidates, with the fit results also shown.

defined as the angle between the momentum of the π^+ (K^0_S) in the $\pi^+\pi^-$ ($K^0_S\pi^+$) rest frame and the momentum of the ρ^0 (K^{*+}) meson in the B^+ rest frame. Following the isobar approach [66], the total amplitude of the $B^+ \to (\pi^+\pi^-)(K^0_S\pi^+)$ consists of the coherent sum of quasi-two-body amplitudes. The differential decay rate for the B^+ decay is defined as the squared modulus of the total amplitude

$$\frac{\mathrm{d}^5\Gamma}{\mathrm{d}(m_{\pi^+\pi^-})\mathrm{d}(m_{K^0_S\pi^+})\mathrm{d}(\cos\theta_{\pi^+\pi^-})\mathrm{d}(\cos\theta_{K^0_S\pi^+})\mathrm{d}\phi} \propto \Phi \times \left|\sum_{i=1}^{N} A_i \times g_i(\cos\theta_{\pi^+\pi^-},\cos\theta_{K^0_S\pi^+},\phi)\times M_i(m_{\pi^+\pi^-},m_{K^0_S\pi^+})\right|^2, \quad (1)$$

where Φ is the four-body phase-space density and A_i is the complex coupling for each amplitude. By construction, the interference terms between components with different spin-parity quantum numbers cancel when integrating over the phase space. For the B^- decay, the sign of the ϕ angle is flipped and an independent set of complex couplings, $\bar{A}_i$, is measured. The g_i functions are characterized by spherical harmonics describing the angular distribution. The 22 amplitudes included in the baseline fit are detailed in Supplemental Material [67]. The M_i functions describe the mass distributions of the $\pi^+\pi^-$ and $K^0_S\pi^+$ systems. They are briefly described below and detailed in Supplemental Material [67].

In the $\pi^+\pi^-$ mass spectrum, besides the $\rho(770)^0$ meson, a few other resonances are identified, including the $\omega(782)$, $f_0(500)$, $f_0(980)$, and $f_0(1370)$ mesons. The mass distributions of the vector resonances, $\rho(770)^0$ and $\omega(782)$, are modeled by a Gounaris-Sakurai parametrization [68] and a relativistic Breit-Wigner function, respectively. Those for the scalar resonances, $f_0(500)$ and $f_0(1370)$, are described by relativistic Breit-Wigner functions, while that for the $f_0(980)$ meson is modeled by a Flatté parametrization [69–71]. Several fits were performed with and without the scalar f_0 states; all states included in the baseline fit have an individual significance above 6 standard deviations. Alternative descriptions of the $\pi\pi$ S wave using the K-matrix formalism are considered as a source of systematic uncertainty, which is detailed below.

The $K^0_S\pi^+$ mass distribution is dominated by the $K^*(892)^+$ resonance and a scalar contribution, referred to as the $(K^0_S\pi^+)_S$ component. The $K^*(892)^+$ resonance is described by a relativistic Breit-Wigner. The $(K^0_S\pi^+)_S$ distribution is parametrized by the LASS [72] model, which includes the contributions of the $K^*_0(1430)^+$ resonance and a broad low-mass component. Possible $(K^0_S\pi^+)_P$ contributions from the $K_1(1270)$, $K_1(1400)$, and $K^*_1(1410)$ states were considered, but no significant effects are expected in the studied mass range. A small fraction of $B^+ \to a_1(1260)^+K^0_S$ and $B^+ \to a_1(1640)^+K^0_S$ decays is observed in the sample, with $a_1^+ \to \rho^0(\to \pi^+\pi^-)\pi^+$, $a_1^+ \to f_0(500)(\to \pi^+\pi^-)\pi^+$, and $a_1^+ \to f_0(980)(\to \pi^+\pi^-)\pi^+$. The a_1 mass distributions are described by relativistic Breit-Wigner functions, with the angular variables redefined accordingly. Parameters describing the mass distributions are fixed in the baseline fit according to the results of previous measurements [15,38].

The combined probability-density function (PDF) for B^+ and B^- decays, composed of signal and background components, is given by

$$\mathcal{P}_{\mathrm{tot}}(\vec{\mathcal{O}},q;\{A_i,\bar{A}_i\}) = \frac{(1+q)\mathcal{P}_{\mathrm{s}}+(1-q)\bar{\mathcal{P}}_{\mathrm{s}}}{2\int(\mathcal{P}_{\mathrm{s}}+\bar{\mathcal{P}}_{\mathrm{s}})\mathrm{d}\vec{\mathcal{O}}}(1-r^+_{\mathrm{b}}-r^-_{\mathrm{b}}) + \frac{(1+q)\mathcal{P}_{\mathrm{b}}}{2\int\mathcal{P}_{\mathrm{b}}\mathrm{d}\vec{\mathcal{O}}}r^+_{\mathrm{b}} + \frac{(1-q)\bar{\mathcal{P}}_{\mathrm{b}}}{2\int\bar{\mathcal{P}}_{\mathrm{b}}\mathrm{d}\vec{\mathcal{O}}}r^-_{\mathrm{b}}, \quad (2)$$

where $q = \pm 1$ indicates the charge of the $B^{\pm}$ meson, and $r_{\rm b}^{\pm}$ are background fractions fixed to the values obtained from the mass fit. The component $\mathcal{P}_{\rm s}$ ($\bar{\mathcal{P}}_{\rm s}$) is the differential decay rate described in Eq. (1) multiplied by the experimental efficiency for the B^+ (B^-) decay. The efficiency map as a function of the five kinematic variables is obtained by parametrizing the simulation sample using five-dimensional Legendre polynomials. Data-driven corrections are applied to the simulation to account for imperfections in the detector response and asymmetries in the detection efficiency of π^+ and π^- tracks. The background distributions, $\mathcal{P}_{\rm b}$ and $\bar{\mathcal{P}}_{\rm b}$, for B^+ and B^- candidates, respectively, are parametrized by five-dimensional Legendre polynomials using candidates in the high-mass region of the $B^{\pm}$ spectra. The amplitude fit is performed simultaneously to the Run 1 and Run 2 samples. In the fit, the phase of each amplitude is measured relative to that of the $B^+ \to \rho^0(K^0_{\rm S}\pi^+)_S$ component, which has a relatively large contribution. As the phase difference between B^+ and B^- is not observable, the phase of the $B^- \to \rho^0(K^0_{\rm S}\pi^-)_S$ component is set to zero. The one-dimensional projections of the amplitude fit in the five kinematic variables are shown in Fig. 2. The CP asymmetry between the couplings of the $B^+ \to \rho^0(K^0_{\rm S}\pi^+)_S$

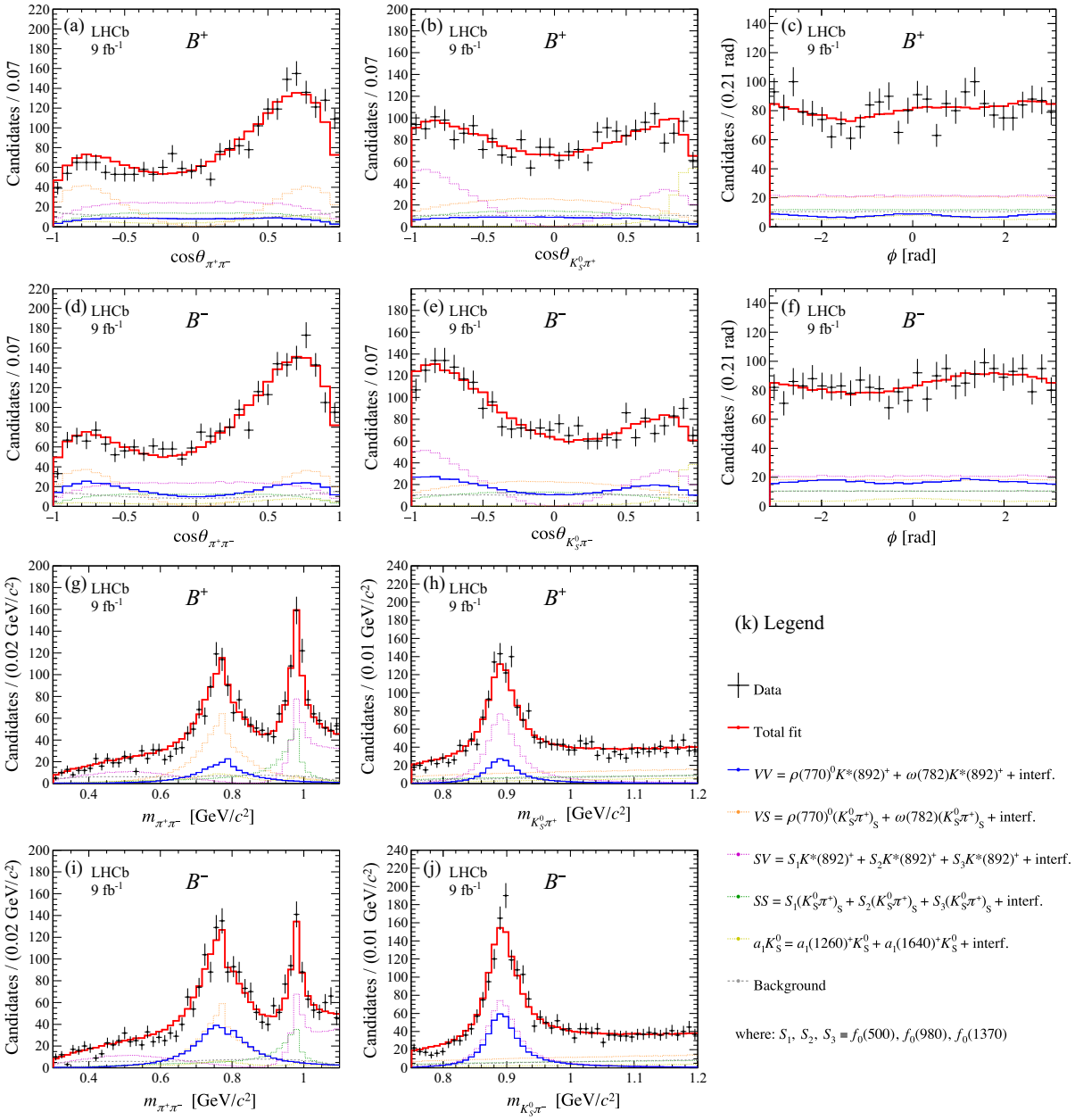

FIG. 2. Projections of the multidimensional amplitude fit onto (a) $\cos\theta_{\pi^+\pi^-}$, (b) $\cos\theta_{K^0_{\rm S}\pi^+}$, (c) ϕ, (g) $m_{\pi^+\pi^-}$, and (h) $m_{K^0_{\rm S}\pi^+}$ for the $B^+ \to (\pi^+\pi^-)(K^0_{\rm S}\pi^+)$ decay. Plots (d)–(f),(i),(j) show the corresponding variables for the $B^- \to (\pi^-\pi^+)(K^0_{\rm S}\pi^-)$ decay.

amplitude and its charge conjugate is found to be consistent with zero.

Two main categories of systematic uncertainty contribute to the result: those originating from experimental assumptions and those related to the amplitude model. The experimental category includes effects due to the limited precision of the background fractions, the efficiency map, and background modeling. The amplitude model uncertainties arise from limited knowledge of the fixed parameters of the resonance mass models, and possible spin-2 components neglected in the baseline fit. Systematic uncertainties due to experimental effects are found to be subdominant. The breakdown of the systematic uncertainties of observables is detailed in Table I of the End Matter. Results of the fitted parameters with their uncertainties are also summarized in Table II of the End Matter.

The experimental systematic uncertainty from the background fractions is evaluated by varying the $r_b^{\pm}$ parameters within their uncertainties and repeating the amplitude fit. Systematic uncertainties due to the efficiency parametrization arise from imperfections of the five-dimensional efficiency map and from any residual charge-asymmetry effect. Imperfections are corrected by a weighting procedure to improve agreement with simulation across the five-dimensional space. The charge-asymmetry effects are assessed by deriving separate efficiency models for B^+ and B^- decays. To evaluate the uncertainty due to the background PDF, an alternative parametrization is obtained by combining B^+ and B^- samples or using samples with more relaxed selection criteria. Also, pseudoexperiments by bootstrapping the background sample [73] are used to extract the background PDF, where for each pseudoexperiment the amplitude fit is performed again. In each case, the deviation from the baseline result or the standard deviation of the results among the pseudoexperiments is taken as the corresponding systematic uncertainty.

The systematic uncertainty due to fixed parameters in the amplitude model is estimated using repeated fits to the data. Each time, the masses, widths, and hadron radii of intermediate resonances are varied within their uncertainties and an amplitude fit is performed under this model. The standard deviation of the distribution of the fit results among the repeated fits is taken as the corresponding systematic uncertainty. For the $B \to VV$ decay, the relative orbital angular momentum of the two vector mesons, L, could take the values $L = 0$ or $L = 2$ for the A_0 and $A_\parallel$ amplitudes, and $L = 1$ for the $A_\perp$ amplitude. Various L configurations are studied and the results are compared with that of the baseline fit with $L = 0$, and the largest difference is taken as the systematic uncertainty. The scalar component of the $\pi^+\pi^-$ mass spectrum can also be modeled using the K-matrix approach [74], as detailed in [75]. The difference between the results obtained with this alternative model and those from the baseline fit using explicit f_0 resonances is taken as a systematic uncertainty. Furthermore, possible contributions of spin-2 resonances to the decay are assessed by including the $f_2(1270) \to \pi^+\pi^-$ or $K_2^*(1430)^+ \to K_S^0\pi^+$ components in the fit. The systematic uncertainties are estimated using the mean value of deviations, between the fits using extended model and baseline model, over an ensemble of pseudoexperiments.

The longitudinal polarization fraction averaged over the $B^+ \to \rho^0 K^{*+}$ and $B^- \to \rho^0 K^{*-}$ final states is determined in terms of the A_λ and $\bar{A}_\lambda$ amplitudes, with $\lambda \in \{0, \parallel, \perp\}$, to be

$$f_L \equiv \frac{|A_0|^2 + |\bar{A}_0|^2}{\sum_\lambda (|A_\lambda|^2 + |\bar{A}_\lambda|^2)} = 0.720 \pm 0.028 \pm 0.009,$$

where, throughout this Letter, the first uncertainty is statistical and the second is systematic. The result is consistent with and more precise than the previous measurement [37]. The charge-specific quantities are determined to be

$$f_L^+ \equiv \frac{|A_0|^2}{\sum_\lambda |A_\lambda|^2} = 0.491 \pm 0.083 \pm 0.025,$$
$$f_L^- \equiv \frac{|\bar{A}_0|^2}{\sum_\lambda |\bar{A}_\lambda|^2} = 0.794 \pm 0.025 \pm 0.006.$$

The direct CP asymmetry for the total $B^+ \to \rho^0 K^{*+}$ decay rates [24,46] is measured to be

$$\mathcal{A}_{CP} \equiv \frac{\sum_\lambda (|\bar{A}_\lambda|^2 - |A_\lambda|^2)}{\sum_\lambda (|\bar{A}_\lambda|^2 + |A_\lambda|^2)} = 0.507 \pm 0.062 \pm 0.024.$$

The CP asymmetries are also determined for the magnitude and phase of each $B^+ \to \rho^0 K^{*+}$ amplitude. The results for the longitudinal component are

$$\mathcal{A}_{CP}(A_0) \equiv \frac{|\bar{A}_0|^2 - |A_0|^2}{|\bar{A}_0|^2 + |A_0|^2} = 0.664 \pm 0.083 \pm 0.029,$$
$$\Delta_{CP}(A_0) \equiv \arg(\bar{A}_0) - \arg(A_0) = 0.720 \pm 0.177 \pm 0.048 \text{ rad},$$

while the CP asymmetries of squared magnitudes and phases of $A_\parallel$ and $A_\perp$ components are measured to be

$$\mathcal{A}_{CP}(A_\parallel) = -0.063 \pm 0.137 \pm 0.027,$$
$$\Delta_{CP}(A_\parallel) = 0.477 \pm 0.187 \pm 0.114 \text{ rad},$$
$$\mathcal{A}_{CP}(A_\perp) = 0.284 \pm 0.140 \pm 0.051,$$
$$\Delta_{CP}(A_\perp) = 0.412 \pm 0.180 \pm 0.122 \text{ rad}.$$

Specifically, sizeable CP violation is observed for the magnitude of the longitudinal component, which drives the CP violation of the overall $B^+ \to \rho^0 K^{*+}$ decay rate. The phase difference between the longitudinal component of the $B^+ \to \rho^0 K^{*+}$ decay and its charge conjugate is 3.9 standard deviations away from zero, which suggests that

long-distance final-state interactions with other contributions in the phase space are playing a role in CP violation. The significance of CP violation for the $B^+ \to \rho^0 K^{*+}$ decay is quantified using a likelihood-ratio test [76] between the baseline fit, which allows for CP violation, and a CP-conserving model where the couplings of the $B^+ \to \rho^0 K^{*+}$ decay and its charge conjugate are constrained to be identical. The significance of a nonvanishing CP asymmetry is found to be above 9 standard deviations with systematic uncertainties taken into account. It marks the first observation of CP violation in this decay.

Triple product asymmetries (TPAs), which exploit the interference between two amplitudes, have been widely used to study CP violation for multibody decays. They are defined to be odd under both the time reversal and parity transformations. A nonzero TPA can either be due to a CP-violating phase or a CP-conserving phase induced by final-state interactions, referred to as the "true" and "fake" TPA, respectively. The true and fake TPAs are related to the couplings of the amplitudes [44,77] as

$$\mathcal{A}^{(1)}_{\substack{\text{true}\\\text{fake}}} \equiv -\frac{2\sqrt{2}}{\pi}\frac{\mathcal{I}m(A_\perp A_0^* \mp \bar{A}_\perp \bar{A}_0^*)}{\sum_{\lambda\in\{0,\parallel,\perp\}}(|A_\lambda|^2+|\bar{A}_\lambda|^2)},$$
$$\mathcal{A}^{(2)}_{\substack{\text{true}\\\text{fake}}} \equiv -\frac{4}{\pi}\frac{\mathcal{I}m(A_\perp A_\parallel^* \mp \bar{A}_\perp \bar{A}_\parallel^*)}{\sum_{\lambda\in\{0,\parallel,\perp\}}(|A_\lambda|^2+|\bar{A}_\lambda|^2)}, \tag{3}$$

where A_λ^* ($\bar{A}_\lambda^*$) denotes the complex conjugate of A_λ ($\bar{A}_\lambda$). Using the amplitude fit results, the TPAs are computed to be

$$\mathcal{A}^{(1)}_{\text{true}} = -0.105 \pm 0.024 \pm 0.013,$$
$$\mathcal{A}^{(2)}_{\text{true}} = 0.007 \pm 0.019 \pm 0.003,$$
$$\mathcal{A}^{(1)}_{\text{fake}} = -0.157 \pm 0.024 \pm 0.011,$$
$$\mathcal{A}^{(2)}_{\text{fake}} = 0.008 \pm 0.018 \pm 0.004.$$

The true TPA $\mathcal{A}^{(1)}_{\text{true}}$ deviates from zero with a significance of approximately 4 standard deviations, indicating evidence of CP violation in interference. The fake TPA $\mathcal{A}^{(1)}_{\text{fake}}$ is nonzero with a significance of about 6 standard deviations, marking parity violation in interference [78].

In summary, an amplitude analysis of the decay $B^+ \to (\pi^+\pi^-)(K^0_S\pi^+)$ is performed within the mass ranges $0.30 < m_{\pi^+\pi^-} < 1.10$ GeV/c^2 and $0.75 < m_{K^0_S\pi^+} < 1.20$ GeV/c^2. The longitudinal polarization and CP asymmetries are studied for the $B^+ \to \rho(770)^0 K^*(892)^+$ decay. The CP-averaged longitudinal fraction is measured to be $f_L = 0.720 \pm 0.028(\text{stat}) \pm 0.009(\text{syst})$. The direct CP asymmetry is determined to be $\mathcal{A}_{CP} = 0.507 \pm 0.062(\text{stat}) \pm 0.024(\text{syst})$, and the significance of CP violation is measured to exceed 9 standard deviations using a likelihood-ratio test. This is the first observation of CP violation in the $B^+ \to \rho(770)^0 K^*(892)^+$ decay. These measurements are consistent with those previously reported by the *BABAR* Collaboration [37], with much better precision. The CP asymmetries are also derived for the magnitudes and phases of the three subamplitudes, suggesting that the longitudinal component drives the total CP violation. These results help to constrain theoretical models used to calculate B-hadron decays, shed light on the dynamics of heavy-flavor decays and contribute to the understanding of the polarization puzzle of B-meson decays.

Acknowledgments—We express our gratitude to our colleagues in the CERN accelerator departments for the excellent performance of the LHC. We thank the technical and administrative staff at the LHCb institutes. We acknowledge support from CERN and from the national agencies: ARC (Australia); CAPES, CNPq, FAPERJ, and FINEP (Brazil); MOST and NSFC (China); CNRS/IN2P3 (France); BMBF, DFG, and MPG (Germany); INFN (Italy); NWO (Netherlands); MNiSW and NCN (Poland); MCID/IFA (Romania); MICIU and AEI (Spain); SNSF and SER (Switzerland); NASU (Ukraine); STFC (United Kingdom); DOE NP and NSF (USA). We acknowledge the computing resources that are provided by ARDC (Australia), CBPF (Brazil), CERN, IHEP and LZU (China), IN2P3 (France), KIT and DESY (Germany), INFN (Italy), SURF (Netherlands), Polish WLCG (Poland), IFIN-HH (Romania), PIC (Spain), CSCS (Switzerland), and GridPP (United Kingdom). We are indebted to the communities behind the multiple open-source software packages on which we depend. Individual groups or members have received support from Key Research Program of Frontier Sciences of CAS, CAS PIFI, CAS CCEPP, Fundamental Research Funds for the Central Universities, and Sci. & Tech. Program of Guangzhou (China); Minciencias (Colombia); EPLANET, Marie Skłodowska-Curie Actions, ERC and NextGenerationEU (European Union); A*MIDEX, ANR, IPhU, and Labex P2IO, and Région Auvergne-Rhône-Alpes (France); Alexander-von-Humboldt Foundation (Germany); ICSC (Italy); Severo Ochoa and María de Maeztu Units of Excellence, GVA, XuntaGal, GENCAT, InTalent-Inditex and Prog. Atracción Talento CM (Spain); SRC (Sweden); the Leverhulme Trust, the Royal Society, and UKRI (United Kingdom).

Data availability—The data that support the findings of this article are openly available [79].

[1] C.-D. Lü, Charmless hadronic B and B_s decays in perturbative QCD approach, Int. J. Mod. Phys. A **23**, 3250 (2008).
[2] M. Beneke, J. Rohrer, and D. Yang, Branching fractions, polarisation and asymmetries of $B \to VV$ decays, Nucl. Phys. **B774**, 64 (2007).

[3] J. G. Körner and G. R. Goldstein, Quark and particle helicities in hadronic charmed particle decays, Phys. Lett. **B89**, 105 (1979).

[4] J. Zhang *et al.* (Belle Collaboration), Observation of $B^{\mp} \to \rho^{\mp}\rho^{0}$ decays, Phys. Rev. Lett. **91**, 221801 (2003).

[5] J. Zhang *et al.* (Belle Collaboration), Measurements of the branching fraction and polarization in $B^{+} \to \rho^{+}K^{*0}$ decays, Phys. Rev. Lett. **95**, 141801 (2005).

[6] K.-F. Chen *et al.* (Belle Collaboration), Measurement of polarization and triple-product correlations in $B \to \phi K^{*}$ decays, Phys. Rev. Lett. **94**, 221804 (2005).

[7] P. Goldenzweig *et al.* (Belle Collaboration), Evidence for neutral B meson decays to ωK^{*0}, Phys. Rev. Lett. **101**, 231801 (2008).

[8] M. Prim *et al.* (Belle Collaboration), Angular analysis of $B^{0} \to \phi K^{*}$ decays and search for CP violation at Belle, Phys. Rev. D **88**, 072004 (2013).

[9] Y. M. Goh *et al.* (Belle Collaboration), Search for the decay $B^{+} \to \bar{K}^{*0}K^{*+}$ at Belle, Phys. Rev. D **91**, 071101 (2015).

[10] P. Vanhoefer *et al.* (Belle Collaboration), Study of $B^{0} \to \rho^{+}\rho^{-}$ decays and implications for the CKM angle ϕ_2, Phys. Rev. D **93**, 032010 (2016); **94**, 099903(E) (2016).

[11] R. Aaij *et al.* (LHCb Collaboration), First observation of the decay $B_s^0 \to \phi\bar{K}^{*0}$, J. High Energy Phys. 11 (2013) 092.

[12] R. Aaij *et al.* (LHCb Collaboration), Measurement of polarization amplitudes and CP asymmetries in $B^{0} \to \phi K^{*}(892)^{0}$, J. High Energy Phys. 05 (2014) 069.

[13] R. Aaij *et al.* (LHCb Collaboration), Observation of the $B^{0} \to \rho^{0}\rho^{0}$ decay from an amplitude analysis of $B^{0} \to (\pi^{+}\pi^{-})(\pi^{+}\pi^{-})$ decays, Phys. Lett. B **747**, 468 (2015).

[14] R. Aaij *et al.* (LHCb Collaboration), First measurement of the CP-violating phase $\phi_s^{d\bar{d}}$ in $B_s^0 \to (K^{+}\pi^{-})(K^{-}\pi^{+})$ decays, J. High Energy Phys. 03 (2018) 140.

[15] R. Aaij *et al.* (LHCb Collaboration), Study of the $B^{0} \to \rho(770)^{0}K^{*}(892)^{0}$ decay with an amplitude analysis of $B^{0} \to (\pi^{+}\pi^{-})(K^{+}\pi^{-})$ decays, J. High Energy Phys. 05 (2019) 026.

[16] R. Aaij *et al.* (LHCb Collaboration), Amplitude analysis of the $B_{(s)}^0 \to K^{*0}\bar{K}^{*0}$ decays and measurement of the branching fraction of the $B^{0} \to K^{*0}\bar{K}^{*0}$ decay, J. High Energy Phys. 07 (2019) 032.

[17] R. Aaij *et al.* (LHCb Collaboration), Measurement of CP violation in the $B_s^0 \to \phi\phi$ decay and search for the $B^{0} \to \phi\phi$ decay, J. High Energy Phys. 12 (2019) 155.

[18] H.-n. Li, Resolution to the $B \to \phi K^{*}$ polarization puzzle, Phys. Lett. B **622**, 63 (2005).

[19] A. L. Kagan, Polarization in $B \to VV$ decays, Phys. Lett. B **601**, 151 (2004).

[20] H.-W. Huang, C.-D. Lü, T. Morii, Y.-L. Shen, G.-L. Song, and J. Zhu, Study of $B \to K^{*}\rho$, $K^{*}\omega$ decays with polarization in the perturbative QCD approach, Phys. Rev. D **73**, 014011 (2006).

[21] F. Su, Y.-L. Wu, Y.-B. Yang, and C. Zhuang, Charmless $B \to PP$, PV, VV decays based on the six-quark effective Hamiltonian with strong phase effects: I, J. Phys. G **38**, 015006 (2011).

[22] C. Wang, Q.-A. Zhang, Y. Li, and C.-D. Lü, Charmless $B_{(s)} \to VV$ decays in factorization-assisted topological-amplitude approach, Eur. Phys. J. C **77**, 333 (2017).

[23] C. W. Bauer, D. Pirjol, I. Z. Rothstein, and I. W. Stewart, $B \to M_1M_2$: Factorization, charming penguins, strong phases, and polarization, Phys. Rev. D **70**, 054015 (2004).

[24] C. Wang, S.-H. Zhou, Y. Li, and C.-D. Lü, Global analysis of charmless B decays into two vector mesons in soft-collinear effective theory, Phys. Rev. D **96**, 073004 (2017).

[25] Z.-T. Zou, A. Ali, C.-D. Lü, X. Liu, and Y. Li, Improved estimates of the $B_{(s)} \to VV$ decays in perturbative QCD approach, Phys. Rev. D **91**, 054033 (2015).

[26] D.-C. Yan, X. Liu, and Z.-J. Xiao, Anatomy of $B_s \to VV$ decays and effects of next-to-leading order contributions in the perturbative QCD factorization approach, Nucl. Phys. **B935**, 17 (2018).

[27] P. Colangelo, F. De Fazio, and T. N. Pham, The riddle of polarization in $B \to VV$ transitions, Phys. Lett. B **597**, 291 (2004).

[28] H.-n. Li and S. Mishima, Polarizations in $B \to VV$ decays, Phys. Rev. D **71**, 054025 (2005).

[29] H.-Y. Cheng, C.-K. Chua, and A. Soni, Final state interactions in hadronic B decays, Phys. Rev. D **71**, 014030 (2005).

[30] M. Ladisa, V. Laporta, G. Nardulli, and P. Santorelli, Final state interactions for $B \to VV$ charmless decays, Phys. Rev. D **70**, 114025 (2004).

[31] Y.-D. Yang, R.-M. Wang, and G.-R. Lu, Polarizations in decays $B_{u,d} \to VV$ and possible implications for R-parity violating supersymmetry, Phys. Rev. D **72**, 015009 (2005).

[32] S. Baek, A. Datta, P. Hamel, O. F. Hernández, and D. London, Polarization states in $B \to \rho K^{*}$ and new physics, Phys. Rev. D **72**, 094008 (2005).

[33] C.-S. Huang, P. Ko, X.-H. Wu, and Y.-D. Yang, MSSM anatomy of the polarization puzzle in $B \to \phi K^{*}$ decays, Phys. Rev. D **73**, 034026 (2006).

[34] S.-S. Bao, F. Su, Y.-L. Wu, and C. Zhuang, Exclusive $B \to VV$ decays and CP violation in the general two-Higgs-doublet model, Phys. Rev. D **77**, 095004 (2008).

[35] C. S. Kim, Sechul Oh, . Sharma, R. Sinha, and Y. W. Yoon, Generalized analysis on $B \to K^{*}\rho$ within and beyond the standard model: Can it help understand the $B \to K\pi$ puzzle?, Phys. Rev. D **76**, 074019 (2007).

[36] A. Datta and D. London, Triple-product correlations in $B \to V_1V_2$ decays and new physics, Int. J. Mod. Phys. A **19**, 2505 (2004).

[37] P. del Amo Sanchez *et al.* (*BABAR* Collaboration), Measurements of branching fractions, polarizations, and direct CP-violation asymmetries in $B^{+} \to \rho^{0}K^{*+}$ and $B^{+} \to f_0(980)K^{*+}$ decays, Phys. Rev. D **83**, 051101 (2011).

[38] S. Navas *et al.* (Particle Data Group), Review of particle physics, Phys. Rev. D **110**, 030001 (2024).

[39] B. Aubert *et al.* (*BABAR* Collaboration), Measurements of branching fractions, polarizations, and direct CP-violation asymmetries in $B \to \rho K^{*}$ and $B \to f_0(980)K^{*}$ decays, Phys. Rev. Lett. **97**, 201801 (2006).

[40] J. P. Lees *et al.* (*BABAR* Collaboration), B^0 meson decays to $\rho^{0}K^{*0}$, f_0K^{*0}, and $\rho^{-}K^{*+}$, including higher K^{*} resonances, Phys. Rev. D **85**, 072005 (2012).

[41] H.-Y. Cheng and K.-C. Yang, Branching ratios and polarization in $B \to VV$, VA, AA decays, Phys. Rev. D **78**, 094001 (2008); **79**, 039903(E) (2009).

[42] H.-Y. Cheng and C.-K. Chua, Revisiting charmless hadronic $B_{u,d}$ decays in QCD factorization, Phys. Rev. D **80**, 114008 (2009).
[43] A. Ali, G. Kramer, and C.-D. Lü, *CP*-violating asymmetries in charmless nonleptonic decays $B \to PP$, PV, VV in the factorization approach, Phys. Rev. D **59**, 014005 (1999).
[44] Y. Li, D.-C. Yan, Z. Rui, and Z.-J. Xiao, Study of $B_{(s)} \to (\pi\pi)(K\pi)$ decays in the perturbative QCD approach, Eur. Phys. J. C **81**, 806 (2021).
[45] J. Chai, S. Cheng, Y.-h. Ju, D.-C. Yan, C.-D. Lü, and Z.-J. Xiao, Charmless two-body B meson decays in the perturbative QCD factorization approach, Chin. Phys. C **46**, 123103 (2022).
[46] D.-C. Yan, H.-n. Li, Z. Rui, Z.-J. Xiao, and Y. Li, Improved global determination of two-meson distribution amplitudes from multi-body B decays, Eur. Phys. J. C **85**, 444 (2025).
[47] M. Gronau, A precise sum rule among four $B \to K\pi CP$ asymmetries, Phys. Lett. B **627**, 82 (2005).
[48] A. A. Alves, Jr. *et al.* (LHCb Collaboration), The LHCb detector at the LHC, J. Instrum. **3**, S08005 (2008).
[49] LHCb Collaboration, LHCb detector performance, Int. J. Mod. Phys. A **30**, 1530022 (2015).
[50] R. Aaij *et al.*, The LHCb trigger and its performance in 2011, J. Instrum. **8**, P04022 (2013).
[51] R. Aaij *et al.*, Design and performance of the LHCb trigger and full real-time reconstruction in Run 2 of the LHC, J. Instrum. **14**, P04013 (2019).
[52] T. Sjöstrand, S. Mrenna, and P. Skands, A brief introduction to PYTHIA 8.1, Comput. Phys. Commun. **178**, 852 (2008).
[53] T. Sjöstrand, S. Mrenna, and P. Skands, PYTHIA 6.4 physics and manual, J. High Energy Phys. 05 (2006) 026.
[54] I. Belyaev *et al.*, Handling of the generation of primary events in Gauss, the LHCb simulation framework, J. Phys. Conf. Ser. **331**, 032047 (2011).
[55] S. Agostinelli *et al.* (Geant4 Collaboration), Geant4: A simulation toolkit, Nucl. Instrum. Methods Phys. Res., Sect. A **506**, 250 (2003).
[56] J. Allison *et al.* (Geant4 Collaboration), Geant4 developments and applications, IEEE Trans. Nucl. Sci. **53**, 270 (2006).
[57] M. Clemencic, G. Corti, S. Easo, C. R. Jones, S. Miglioranzi, M. Pappagallo, and P. Robbe, The LHCb simulation application, Gauss: Design, evolution and experience, J. Phys. Conf. Ser. **331**, 032023 (2011).
[58] N. Davidson, T. Przedzinski, and Z. Was, PHOTOS interface in C++: Technical and physics documentation, Comput. Phys. Commun. **199**, 86 (2016).
[59] D. J. Lange, The EvtGen particle decay simulation package, Nucl. Instrum. Methods Phys. Res., Sect. A **462**, 152 (2001).
[60] L. Breiman, J. H. Friedman, R. A. Olshen, and C. J. Stone, *Classification and Regression Trees* (Wadsworth International Group, Belmont, CA, 1984).
[61] Y. Freund and R. E. Schapire, A decision-theoretic generalization of on-line learning and an application to boosting, J. Comput. Syst. Sci. **55**, 119 (1997).
[62] H. Voss, A. Hoecker, J. Stelzer, and F. Tegenfeldt, TMVA—Toolkit for multivariate data analysis with ROOT, Proc. Sci. ACAT2007 (**2007**) 040.
[63] A. Hoecker *et al.*, TMVA 4—Toolkit for multivariate data analysis with ROOT. Users guide, arXiv:physics/0703039.
[64] T. Skwarnicki, A study of the radiative cascade transitions between the Upsilon-prime and Upsilon resonances, Ph.D. thesis, Institute of Nuclear Physics, Krakow, 1986; DESY-F31-86-02.
[65] H. Albrecht *et al.* (ARGUS Collaboration), Search for hadronic $b \to u$ decays, Phys. Lett. B **241**, 278 (1990).
[66] D. J. Herndon, P. Söding, and R. J. Cashmore, Generalized isobar model formalism, Phys. Rev. D **11**, 3165 (1975).
[67] See Supplemental Material at http://link.aps.org/supplemental/10.1103/9zhl-kkwg for the complete set of amplitudes with corresponding angular distributions and mass models.
[68] G. J. Gounaris and J. J. Sakurai, Finite-width corrections to the vector-meson-dominance prediction for $\rho \to e^+e^-$, Phys. Rev. Lett. **21**, 244 (1968).
[69] S. M. Flatté, Coupled-channel analysis of the $\pi\eta$ and $K\bar{K}$ systems near $K\bar{K}$ threshold, Phys. Lett. **63B**, 224 (1976).
[70] S. M. Flatté, On the nature of 0^+ mesons, Phys. Lett. **63B**, 228 (1976).
[71] D. V. Bugg, Reanalysis of data on $a_0(1450)$ and $a_0(980)$, Phys. Rev. D **78**, 074023 (2008).
[72] D. Aston *et al.*, A study of $K^-\pi^+$ scattering in the reaction $K^-p \to K^-\pi^+n$ at 11 GeV/c, Nucl. Phys. **B296**, 493 (1988).
[73] B. Efron, Bootstrap methods: Another look at the jackknife, Ann. Stat. **7**, 1 (1979).
[74] S. U. Chung *et al.*, Partial wave analysis in K matrix formalism, Ann. Phys. (N.Y.) **4**, 404 (1995).
[75] J. Back *et al.*, LAURA^{++}: A Dalitz plot fitter, Comput. Phys. Commun. **231**, 198 (2018).
[76] S. S. Wilks, The large-sample distribution of the likelihood ratio for testing composite hypotheses, Ann. Math. Stat. **9**, 60 (1938).
[77] M. Gronau and J. L. Rosner, Triple-product asymmetries in K, $D_{(s)}$ and $B_{(s)}$ decays, Phys. Rev. D **84**, 096013 (2011).
[78] A. Datta, M. Duraisamy, and D. London, Searching for new physics with B-decay fake triple products, Phys. Lett. B **701**, 357 (2011).
[79] https://cds.cern.ch/record/2940533.
[80] R. Barlow, A. R. Brazzale, and I. Volobouev, Asymmetric errors, Nucl. Instrum. Methods Phys. Res., Sect. A **1082**, 170857 (2026).

End Matter

The breakdown of systematic uncertainty contributions for the reported observables is shown in Table I.

Results of the fitted amplitude parameters, i.e., the real and imaginary parts of amplitude couplings, are summarized in Table II. Asymmetric uncertainties are evaluated following the procedure described in Ref. [80]. Parameters marked with "⋯" are constrained in the fit, as explained below.

The reference amplitude is taken to be $A_{\rho(K^0_S\pi)_S}$, with couplings fixed to

TABLE I. Summary of the systematic uncertainty contributions for the reported observables, with statistical and total systematic uncertainties shown as reference. These uncertainties are given as absolute values.

	Statistical	Systematic (total)	Background fractions	Efficiency map	Background modeling	Mass models	Spin-2 components
$\mathcal{A}_{CP}$	0.062	0.024	0.0001	0.0049	0.0066	0.0216	0.0067
$\mathcal{A}_{CP}(A_0)$	0.083	0.029	0.0003	0.0061	0.0114	0.0206	0.0151
$\mathcal{A}_{CP}(A_\parallel)$	0.137	0.027	0.0015	0.0040	0.0175	0.0166	0.0116
$\mathcal{A}_{CP}(A_\perp)$	0.140	0.051	0.0005	0.0035	0.0158	0.0467	0.0116
$\Delta_{CP}(A_0)$	0.177	0.048	0.0031	0.0129	0.0304	0.0314	0.0141
$\Delta_{CP}(A_\parallel)$	0.187	0.114	0.0040	0.0021	0.0138	0.1092	0.0282
$\Delta_{CP}(A_\perp)$	0.180	0.122	0.0013	0.0053	0.0175	0.1145	0.0365

TABLE II. Summary of the fitted real and imaginary parts of the amplitude couplings for the B^+ and B^- samples, respectively. The first uncertainties are statistical and the second ones are systematic. The reference amplitude is taken to be $A_{\rho(K^0_S\pi)_S}$. Parameters for the $a_1^+K^0_S$ components are reduced by constraining the CP-violating contributions to be the same among decay channels for each a_1 resonance, since its subdecays are CP-conserving strong interactions. These are signified with a "$\cdots$" in the table.

Parameter	B^+			B^-		
$\mathcal{R}e(A_{\rho(K^0_S\pi)_S})$		$\cdots$		0.9735	±0.0314	±0.0142
$\mathcal{I}m(A_{\rho(K^0_S\pi)_S})$		0 (Fixed)			0 (Fixed)	
$\mathcal{R}e(A^0_{\rho K^*})$	0.1641	±0.0254	±0.0415	0.2392	±0.0332	±0.0750
$\mathcal{I}m(A^0_{\rho K^*})$	0.0242	±0.0266	±0.0316	0.2811	±0.0326	±0.0779
$\mathcal{R}e(A^\parallel_{\rho K^*})$	-0.1289	±0.0141	±0.0332	-0.1203	±0.0143	±0.0293
$\mathcal{I}m(A^\parallel_{\rho K^*})$	0.0297	±0.0184	±0.0307	-0.0308	±0.0180	±0.0209
$\mathcal{R}e(A^\perp_{\rho K^*})$	-0.1021	±0.0142	±0.0261	-0.1385	±0.0133	±0.0325
$\mathcal{I}m(A^\perp_{\rho K^*})$	0.0246	±0.0160	±0.0249	-0.0246	±0.0174	±0.0248
$\mathcal{R}e(A^0_{\omega K^*})$	0.0005	±0.0067	±0.0059	-0.0087	±0.0056	±0.0034
$\mathcal{I}m(A^0_{\omega K^*})$	-0.0114	±0.0058	±0.0126	-0.0119	±0.0074	±0.0029
$\mathcal{R}e(A^\parallel_{\omega K^*})$	-0.0023	±0.0030	±0.0009	-0.0006	±0.0023	±0.0005
$\mathcal{I}m(A^\parallel_{\omega K^*})$	-0.0025	±0.0028	±0.0013	0.0020	±0.0022	±0.0007
$\mathcal{R}e(A^\perp_{\omega K^*})$	-0.0001	±0.0044	±0.0014	-0.0027	±0.0033	±0.0008
$\mathcal{I}m(A^\perp_{\omega K^*})$	-0.0042	±0.0030	±0.0013	0.0015	±0.0034	±0.0007
$\mathcal{R}e(A_{\omega(K^0_S\pi)_S})$	0.0052	±0.0112	±0.0041	-0.0001	±0.0119	±0.0019
$\mathcal{I}m(A_{\omega(K^0_S\pi)_S})$	0.0254	±0.0096	±0.0048	0.0276	±0.0087	±0.0026
$\mathcal{R}e(A_{f_0(500)K^*})$	1.5539	±0.1852	±0.3636	1.0127	±0.2455	±0.2885
$\mathcal{I}m(A_{f_0(500)K^*})$	0.3152	±0.3778	±0.2541	1.1808	±0.2386	±0.3634
$\mathcal{R}e(A_{f_0(980)K^*})$	-0.1784	$^{+0.0909}_{-0.1102}$	$^{+0.1183}_{-0.1341}$	-0.4046	$^{+0.0667}_{-0.1624}$	$^{+0.0913}_{-0.1537}$
$\mathcal{I}m(A_{f_0(980)K^*})$	-0.6713	$^{+0.0811}_{-0.3013}$	$^{+0.1309}_{-0.1595}$	-0.6048	$^{+0.0824}_{-0.2850}$	$^{+0.1284}_{-0.1519}$
$\mathcal{R}e(A_{f_0(1370)K^*})$	0.5053	$^{+0.3206}_{-0.3195}$	$^{+0.2821}_{-0.2658}$	1.0462	$^{+0.1879}_{-0.2688}$	$^{+0.3300}_{-0.2286}$
$\mathcal{I}m(A_{f_0(1370)K^*})$	0.1557	$^{+0.2860}_{-0.2424}$	$^{+0.1668}_{-0.1855}$	0.4208	$^{+0.2378}_{-0.2555}$	$^{+0.2246}_{-0.2077}$
$\mathcal{R}e(A_{f_0(500)(K^0_S\pi)_S})$	0.6749	±0.4192	±0.2929	1.3057	±0.3611	±0.2671
$\mathcal{I}m(A_{f_0(500)(K^0_S\pi)_S})$	-0.3747	±0.4989	±0.2675	-0.1689	±0.5528	±0.2425
$\mathcal{R}e(A_{f_0(980)(K^0_S\pi)_S})$	-0.2698	$^{+0.0870}_{-0.2642}$	$^{+0.1513}_{-0.1596}$	-0.3532	$^{+0.0924}_{-0.2573}$	$^{+0.0725}_{-0.0790}$
$\mathcal{I}m(A_{f_0(980)(K^0_S\pi)_S})$	1.3567	$^{+0.6411}_{-0.2222}$	$^{+0.3352}_{-0.3304}$	0.9319	$^{+0.4909}_{-0.1349}$	$^{+0.3050}_{-0.3044}$
$\mathcal{R}e(A_{f_0(1370)(K^0_S\pi)_S})$	1.3511	$^{+0.5718}_{-0.5138}$	$^{+0.5271}_{-0.5279}$	0.2864	$^{+0.5436}_{-0.5300}$	$^{+0.4094}_{-0.4008}$
$\mathcal{I}m(A_{f_0(1370)(K^0_S\pi)_S})$	0.1008	$^{+1.0180}_{-0.4300}$	$^{+0.6857}_{-0.6563}$	0.5882	$^{+0.4970}_{-0.4542}$	$^{+0.3376}_{-0.3491}$
$\mathcal{R}e(A^0_{(a_1(1260)\to\rho\pi)K^0_S})$	-2.5802	±1.3487	±2.2671	-2.0785	±0.6787	±0.9635

(Table continued)

TABLE II. *(Continued)*

Parameter		B^+			B^-	
$\mathcal{I}m(A^0_{(a_1(1260)\to\rho\pi)K^0_S})$	-0.5676	±0.9027	±1.1999	-0.8797	±0.6419	±0.8860
$\mathcal{R}e(A^{\parallel}_{(a_1(1260)\to\rho\pi)K^0_S})$		$\cdots$		-0.1507	±1.5943	±0.8448
$\mathcal{I}m(A^{\parallel}_{(a_1(1260)\to\rho\pi)K^0_S})$		$\cdots$		3.0275	±1.3924	±1.4278
$\mathcal{R}e(A_{(a_1(1260)\to f_0(500)\pi)K^0_S})$		$\cdots$		-8.5584	$^{+1.8330}_{-1.8408}$	$^{+4.2256}_{-3.9197}$
$\mathcal{I}m(A_{(a_1(1260)\to f_0(500)\pi)K^0_S})$		$\cdots$		3.5230	$^{+1.2376}_{-0.7814}$	$^{+2.0371}_{-2.0247}$
$\mathcal{R}e(A_{(a_1(1260)\to f_0(980)\pi)K^0_S})$		$\cdots$		1.2407	$^{+0.8240}_{-1.2627}$	$^{+1.3965}_{-1.3885}$
$\mathcal{I}m(A_{(a_1(1260)\to f_0(980)\pi)K^0_S})$		$\cdots$		0.7200	$^{+0.8666}_{-1.0314}$	$^{+0.4065}_{-0.4259}$
$\mathcal{R}e(A^0_{(a_1(1640)\to\rho\pi)K^0_S})$	-0.3555	±0.4472	±0.3954	-0.2564	±0.4432	±0.3951
$\mathcal{I}m(A^0_{(a_1(1640)\to\rho\pi)K^0_S})$	-0.0363	±0.5007	±0.3456	-0.0859	±0.3758	±0.2064
$\mathcal{R}e(A^{\parallel}_{(a_1(1640)\to\rho\pi)K^0_S})$		$\cdots$		-0.3892	±0.8504	±0.5404
$\mathcal{I}m(A^{\parallel}_{(a_1(1640)\to\rho\pi)K^0_S})$		$\cdots$		-0.2174	±0.9290	±0.9068
$\mathcal{R}e(A_{(a_1(1640)\to f_0(500)\pi)K^0_S})$		$\cdots$		3.8584	±1.3145	±1.4161
$\mathcal{I}m(A_{(a_1(1640)\to f_0(500)\pi)K^0_S})$		$\cdots$		0.5558	±1.1537	±1.6115
$\mathcal{R}e(A_{(a_1(1640)\to f_0(980)\pi)K^0_S})$		$\cdots$		-0.3569	$^{+0.6560}_{-0.7193}$	$^{+1.1383}_{-1.1493}$
$\mathcal{I}m(A_{(a_1(1640)\to f_0(980)\pi)K^0_S})$		$\cdots$		-1.7988	$^{+0.6287}_{-0.6458}$	$^{+1.1608}_{-1.1620}$

$$B^+:\ \mathcal{R}e(A^+_{\rho(K^0_S\pi)_S})=1-\Delta,\qquad \mathcal{I}m(A^+_{\rho(K^0_S\pi)_S})=0,$$
$$B^-:\ \mathcal{R}e(A^-_{\rho(K^0_S\pi)_S})=1+\Delta,\qquad \mathcal{I}m(A^-_{\rho(K^0_S\pi)_S})=0, \tag{A1}$$

where Δ describes the CP asymmetry of the reference amplitude. In the fit, $\mathcal{R}e(A^+_{\rho(K^0_S\pi)_S})$ is thus constrained to be $2-\mathcal{R}e(A^-_{\rho(K^0_S\pi)_S})$.

For each a_1 resonance, the decays $a_1\to X\pi$ $[X=\rho, f_0(500), f_0(980)]$ proceed via CP-conserving strong interactions. The CP-violating contributions are therefore shared among all $B\to a_1K^0_S$ channels, where a_1 denotes $a_1(1260)^+$ or $a_1(1640)^+$. The four amplitudes satisfy

$$\frac{A^+_0}{A^-_0}=\frac{A^+_1}{A^-_1}=\frac{A^+_2}{A^-_2}=\frac{A^+_3}{A^-_3}, \tag{A2}$$

with

$$A_0=A^0_{a_1(\to\rho\pi)K^0_S},\qquad A_1=A^{\parallel}_{a_1(\to\rho\pi)K^0_S},$$
$$A_2=A_{a_1(\to f_0(500)\pi)K^0_S},\qquad A_3=A_{a_1(\to f_0(980)\pi)K^0_S}. \tag{A3}$$

In the fit, A^+_0 and all $A^-_{i=0,1,2,3}$ are free parameters, while the other $A^+_{i=1,2,3}$ are constrained through these relations.

R. Aaij,[38] A. S. W. Abdelmotteleb,[57] C. Abellan Beteta,[51] F. Abudinén,[57] T. Ackernley,[61] A. A. Adefisoye,[69] B. Adeva,[47] M. Adinolfi,[55] P. Adlarson,[85] C. Agapopoulou,[14] C. A. Aidala,[87] Z. Ajaltouni,[11] S. Akar,[11] K. Akiba,[38] P. Albicocco,[28] J. Albrecht,[19,b] R. Aleksiejunas,[80] F. Alessio,[49] P. Alvarez Cartelle,[56] R. Amalric,[16] S. Amato,[3] J. L. Amey,[55] Y. Amhis,[14] L. An,[6] L. Anderlini,[27] M. Andersson,[51] P. Andreola,[51] M. Andreotti,[26] S. Andres Estrada,[84] A. Anelli,[31,49,c] D. Ao,[7] C. Arata,[12] F. Archilli,[37,d] Z Areg,[69] M. Argenton,[26] S. Arguedas Cuendis,[9,49] L. Arnone,[31,c] A. Artamonov,[44] M. Artuso,[69] E. Aslanides,[13] R. Ataíde Da Silva,[50] M. Atzeni,[65] B. Audurier,[12] J. A. Authier,[15] D. Bacher,[64] I. Bachiller Perea,[50] S. Bachmann,[22] M. Bachmayer,[50] J. J. Back,[57] P. Baladron Rodriguez,[47] V. Balagura,[15] A. Balboni,[26] W. Baldini,[26] Z. Baldwin,[78] L. Balzani,[19] H. Bao,[7] J. Baptista de Souza Leite,[2] C. Barbero Pretel,[47,12] M. Barbetti,[27] I. R. Barbosa,[70] R. J. Barlow,[63] M. Barnyakov,[25] S. Barsuk,[14] W. Barter,[59] J. Bartz,[69] S. Bashir,[40] B. Batsukh,[5] P. B. Battista,[14] A. Bay,[50] A. Beck,[65] M. Becker,[19] F. Bedeschi,[35] I. B. Bediaga,[2] N. A. Behling,[19] S. Belin,[47] A. Bellavista,[25]

K. Belous,[44] I. Belov,[29] I. Belyaev,[36] G. Benane,[13] G. Bencivenni,[28] E. Ben-Haim,[16] A. Berezhnoy,[44] R. Bernet,[51] S. Bernet Andres,[46] A. Bertolin,[33] C. Betancourt,[51] F. Betti,[59] J. Bex,[56] Ia. Bezshyiko,[51] O. Bezshyyko,[86] J. Bhom,[41] M. S. Bieker,[18] N. V. Biesuz,[26] P. Billoir,[16] A. Biolchini,[38] M. Birch,[62] F. C. R. Bishop,[10] A. Bitadze,[63] A. Bizzeti,[27,e] T. Blake,[57,f] F. Blanc,[50] J. E. Blank,[19] S. Blusk,[69] V. Bocharnikov,[44] J. A. Boelhauve,[19] O. Boente Garcia,[15] T. Boettcher,[68] A. Bohare,[59] A. Boldyrev,[44] C. S. Bolognani,[82] R. Bolzonella,[26,g] R. B. Bonacci,[1] N. Bondar,[44,49] A. Bordelius,[49] F. Borgato,[33,49] S. Borghi,[63] M. Borsato,[31,c] J. T. Borsuk,[83] E. Bottalico,[61] S. A. Bouchiba,[50] M. Bovill,[64] T. J. V. Bowcock,[61] A. Boyer,[49] C. Bozzi,[26] J. D. Brandenburg,[88] A. Brea Rodriguez,[50] N. Breer,[19] J. Brodzicka,[41] A. Brossa Gonzalo,[47,a] J. Brown,[61] D. Brundu,[32] E. Buchanan,[59] M. Burgos Marcos,[82] A. T. Burke,[63] C. Burr,[49] C. Buti,[27] J. S. Butter,[56] J. Buytaert,[49] W. Byczynski,[49] S. Cadeddu,[32] H. Cai,[75] Y. Cai,[5] A. Caillet,[16] R. Calabrese,[26,g] S. Calderon Ramirez,[9] L. Calefice,[45] S. Cali,[28] M. Calvi,[31,c] M. Calvo Gomez,[46] P. Camargo Magalhaes,[2,h] J. I. Cambon Bouzas,[47] P. Campana,[28] D. H. Campora Perez,[82] A. F. Campoverde Quezada,[7] S. Capelli,[31] M. Caporale,[25] L. Capriotti,[26] R. Caravaca-Mora,[9] A. Carbone,[25,i] L. Carcedo Salgado,[47] R. Cardinale,[29,j] A. Cardini,[32] P. Carniti,[31] L. Carus,[22] A. Casais Vidal,[65] R. Caspary,[22] G. Casse,[61] M. Cattaneo,[49] G. Cavallero,[26] V. Cavallini,[26,g] S. Celani,[22] I. Celestino,[35,k] S. Cesare,[30,l] F. Cesario Laterza Lopes,[2] A. J. Chadwick,[61] I. Chahrour,[87] H. Chang,[4,m] M. Charles,[16] Ph. Charpentier,[49] E. Chatzianagnostou,[38] R. Cheaib,[79] M. Chefdeville,[10] C. Chen,[56] J. Chen,[50] S. Chen,[5] Z. Chen,[7] M. Cherif,[12] A. Chernov,[41] S. Chernyshenko,[53] X. Chiotopoulos,[82] V. Chobanova,[84] M. Chrzaszcz,[41] A. Chubykin,[44] V. Chulikov,[28,36,49] P. Ciambrone,[28] X. Cid Vidal,[47] G. Ciezarek,[49] P. Cifra,[38] P. E. L. Clarke,[59] M. Clemencic,[49] H. V. Cliff,[56] J. Closier,[49] C. Cocha Toapaxi,[22] V. Coco,[49] J. Cogan,[13] E. Cogneras,[11] L. Cojocariu,[43] S. Collaviti,[50] P. Collins,[49] T. Colombo,[49] M. Colonna,[19] A. Comerma-Montells,[45] L. Congedo,[24] J. Connaughton,[57] A. Contu,[32] N. Cooke,[60] G. Cordova,[35,k] C. Coronel,[66] I. Corredoira,[12] A. Correia,[16] G. Corti,[49] J. Cottee Meldrum,[55] B. Couturier,[49] D. C. Craik,[51] M. Cruz Torres,[2,n] E. Curras Rivera,[50] R. Currie,[59] C. L. Da Silva,[68] S. Dadabaev,[44] L. Dai,[72] X. Dai,[4] E. Dall'Occo,[49] J. Dalseno,[84] C. D'Ambrosio,[62] J. Daniel,[11] P. d'Argent,[24] G. Darze,[3] A. Davidson,[57] J. E. Davies,[63] O. De Aguiar Francisco,[63] C. De Angelis,[32,o] F. De Benedetti,[49] J. de Boer,[38] K. De Bruyn,[81] S. De Capua,[63] M. De Cian,[63] U. De Freitas Carneiro Da Graca,[2,p] E. De Lucia,[28] J. M. De Miranda,[2] L. De Paula,[3] M. De Serio,[24,q] P. De Simone,[28] F. De Vellis,[19] J. A. de Vries,[82] F. Debernardis,[24] D. Decamp,[10] S. Dekkers,[1] L. Del Buono,[16] B. Delaney,[65] H.-P. Dembinski,[19] J. Deng,[8] V. Denysenko,[51] O. Deschamps,[11] F. Dettori,[32,o] B. Dey,[79] P. Di Nezza,[28] I. Diachkov,[44] S. Didenko,[44] S. Ding,[69] Y. Ding,[50] L. Dittmann,[22] V. Dobishuk,[53] A. D. Docheva,[60] A. Doheny,[57] C. Dong,[4,m] A. M. Donohoe,[23] F. Dordei,[32] A. C. dos Reis,[2] A. D. Dowling,[69] L. Dreyfus,[13] W. Duan,[73] P. Duda,[83] L. Dufour,[49] V. Duk,[34] P. Durante,[49] M. M. Duras,[83] J. M. Durham,[68] O. D. Durmus,[79] A. Dziurda,[41] A. Dzyuba,[44] S. Easo,[58] E. Eckstein,[18] U. Egede,[1] A. Egorychev,[44] V. Egorychev,[44] S. Eisenhardt,[59] E. Ejopu,[61] L. Eklund,[85] M. Elashri,[66] J. Ellbracht,[19] S. Ely,[62] A. Ene,[43] J. Eschle,[69] S. Esen,[22] T. Evans,[38] F. Fabiano,[32] S. Faghih,[66] L. N. Falcao,[2] B. Fang,[7] R. Fantechi,[35] L. Fantini,[34,r] M. Faria,[50] K. Farmer,[59] D. Fazzini,[31,c] L. Felkowski,[83] M. Feng,[5,7] M. Feo,[19] A. Fernandez Casani,[48] M. Fernandez Gomez,[47] A. D. Fernez,[67] F. Ferrari,[25,i] F. Ferreira Rodrigues,[3] M. Ferrillo,[51] M. Ferro-Luzzi,[49] S. Filippov,[44] R. A. Fini,[24] M. Fiorini,[26,g] M. Firlej,[40] K. L. Fischer,[64] D. S. Fitzgerald,[87] C. Fitzpatrick,[63] T. Fiutowski,[40] F. Fleuret,[15] A. Fomin,[52] M. Fontana,[25] L. F. Foreman,[63] R. Forty,[49] D. Foulds-Holt,[59] V. Franco Lima,[3] M. Franco Sevilla,[67] M. Frank,[49] E. Franzoso,[26,g] G. Frau,[63] C. Frei,[49] D. A. Friday,[63,49] J. Fu,[7] Q. Führing,[19,56,b] T. Fulghesu,[13] G. Galati,[24] M. D. Galati,[38] A. Gallas Torreira,[47] D. Galli,[25,i] S. Gambetta,[59] M. Gandelman,[3] P. Gandini,[30] B. Ganie,[63] H. Gao,[7] R. Gao,[64] T. Q. Gao,[56] Y. Gao,[8] Y. Gao,[6] Y. Gao,[8] L. M. Garcia Martin,[50] P. Garcia Moreno,[45] J. García Pardiñas,[65] P. Gardner,[67] K. G. Garg,[8] L. Garrido,[45] C. Gaspar,[49] A. Gavrikov,[33] L. L. Gerken,[19] E. Gersabeck,[20] M. Gersabeck,[20] T. Gershon,[57] S. Ghizzo,[29,j] Z. Ghorbanimoghaddam,[55] L. Giambastiani,[33,s] F. I. Giasemis,[16,t] V. Gibson,[56] H. K. Giemza,[42] A. L. Gilman,[64] M. Giovannetti,[28] A. Gioventù,[45] L. Girardey,[63,58] M. A. Giza,[41] F. C. Glaser,[14,22] V. V. Gligorov,[16] C. Göbel,[70] L. Golinka-Bezshyyko,[86] E. Golobardes,[46] D. Golubkov,[44] A. Golutvin,[62,49] S. Gomez Fernandez,[45] W. Gomulka,[40] I. Gonçales Vaz,[49] F. Goncalves Abrantes,[64] M. Goncerz,[41] G. Gong,[4,m] J. A. Gooding,[19] I. V. Gorelov,[44] C. Gotti,[31] E. Govorkova,[65] J. P. Grabowski,[18]

L. A. Granado Cardoso,[49] E. Graugés,[45] E. Graverini,[50,u] L. Grazette,[57] G. Graziani,[27] A. T. Grecu,[43] L. M. Greeven,[38] N. A. Grieser,[66] L. Grillo,[60] S. Gromov,[44] C. Gu,[15] M. Guarise,[26] L. Guerry,[11] V. Guliaeva,[44] P. A. Günther,[22] A.-K. Guseinov,[50] E. Gushchin,[44] Y. Guz,[6,49] T. Gys,[49] K. Habermann,[18] T. Hadavizadeh,[1] C. Hadjivasiliou,[67] G. Haefeli,[50] C. Haen,[49] S. Haken,[56] G. Hallett,[57] P. M. Hamilton,[67] J. Hammerich,[61] Q. Han,[33] X. Han,[22,49] S. Hansmann-Menzemer,[22] L. Hao,[7] N. Harnew,[64] T. H. Harris,[1] M. Hartmann,[14] S. Hashmi,[40] J. He,[7,v] A. Hedes,[63] F. Hemmer,[49] C. Henderson,[66] R. Henderson,[14] R. D. L. Henderson,[1] A. M. Hennequin,[49] K. Hennessy,[61] L. Henry,[50] J. Herd,[62] P. Herrero Gascon,[22] J. Heuel,[17] A. Hicheur,[3] G. Hijano Mendizabal,[51] J. Horswill,[63] R. Hou,[8] Y. Hou,[11] D. C. Houston,[60] N. Howarth,[61] J. Hu,[73] W. Hu,[7] X. Hu,[4,m] W. Hulsbergen,[38] R. J. Hunter,[57] M. Hushchyn,[44] D. Hutchcroft,[61] M. Idzik,[40] D. Ilin,[44] P. Ilten,[66] A. Iniukhin,[44] A. Iohner,[10] A. Ishteev,[44] K. Ivshin,[44] H. Jage,[17] S. J. Jaimes Elles,[77,48,49] S. Jakobsen,[49] E. Jans,[38] B. K. Jashal,[48] A. Jawahery,[67] C. Jayaweera,[54] V. Jevtic,[19] Z. Jia,[16] E. Jiang,[67] X. Jiang,[5,7] Y. Jiang,[7] Y. J. Jiang,[6] E. Jimenez Moya,[9] N. Jindal,[88] M. John,[64] A. John Rubesh Rajan,[23] D. Johnson,[54] C. R. Jones,[56] S. Joshi,[42] B. Jost,[49] J. Juan Castella,[56] N. Jurik,[49] I. Juszczak,[41] D. Kaminaris,[50] S. Kandybei,[52] M. Kane,[59] Y. Kang,[4,m] C. Kar,[11] M. Karacson,[49] A. Kauniskangas,[50] J. W. Kautz,[66] M. K. Kazanecki,[41] F. Keizer,[49] M. Kenzie,[56] T. Ketel,[38] B. Khanji,[69] A. Kharisova,[44] S. Kholodenko,[62,49] G. Khreich,[14] T. Kirn,[17] V. S. Kirsebom,[31,c] O. Kitouni,[65] S. Klaver,[39] N. Kleijne,[35,k] D. K. Klekots,[86] K. Klimaszewski,[42] M. R. Kmiec,[42] T. Knospe,[19] S. Koliiev,[53] L. Kolk,[19] A. Konoplyannikov,[6] P. Kopciewicz,[49] P. Koppenburg,[38] A. Korchin,[52] M. Korolev,[44] I. Kostiuk,[38] O. Kot,[53] S. Kotriakhova, E. Kowalczyk,[67] A. Kozachuk,[44] P. Kravchenko,[44] L. Kravchuk,[44] O. Kravcov,[80] M. Kreps,[57] P. Krokovny,[44] W. Krupa,[69] W. Krzemien,[42] O. Kshyvanskyi,[53] S. Kubis,[83] M. Kucharczyk,[41] V. Kudryavtsev,[44] E. Kulikova,[44] A. Kupsc,[85] V. Kushnir,[52] B. Kutsenko,[13] J. Kvapil,[68] I. Kyryllin,[52] D. Lacarrere,[49] P. Laguarta Gonzalez,[45] A. Lai,[32] A. Lampis,[32] D. Lancierini,[62] C. Landesa Gomez,[47] J. J. Lane,[1] G. Lanfranchi,[28] C. Langenbruch,[22] J. Langer,[19] O. Lantwin,[44] T. Latham,[57] F. Lazzari,[35,49,u] C. Lazzeroni,[54] R. Le Gac,[13] H. Lee,[61] R. Lefèvre,[11] A. Leflat,[44] S. Legotin,[44] M. Lehuraux,[57] E. Lemos Cid,[49] O. Leroy,[13] T. Lesiak,[41] E. D. Lesser,[49] B. Leverington,[22] A. Li,[4,m] C. Li,[4] C. Li,[13] H. Li,[73] J. Li,[8] K. Li,[76] L. Li,[63] M. Li,[8] P. Li,[7] P.-R. Li,[74] Q. Li,[5,7] T. Li,[72] T. Li,[73] Y. Li,[8] Y. Li,[5] Y. Li,[4] Z. Lian,[4,m] Q. Liang,[8] X. Liang,[69] Z. Liang,[32] S. Libralon,[48] A. L. Lightbody,[12] C. Lin,[7] T. Lin,[58] R. Lindner,[49] H. Linton,[62] R. Litvinov,[32] D. Liu,[8] F. L. Liu,[1] G. Liu,[73] K. Liu,[74] S. Liu,[5,7] W. Liu,[8] Y. Liu,[59] Y. Liu,[74] Y. L. Liu,[62] G. Loachamin Ordonez,[70] A. Lobo Salvia,[45] A. Loi,[32] T. Long,[56] J. H. Lopes,[3] A. Lopez Huertas,[45] C. Lopez Iribarnegaray,[47] S. López Soliño,[47] Q. Lu,[15] C. Lucarelli,[49] D. Lucchesi,[33,s] M. Lucio Martinez,[48] Y. Luo,[6] A. Lupato,[33,w] E. Luppi,[26,g] K. Lynch,[23] X.-R. Lyu,[7] G. M. Ma,[4,m] S. Maccolini,[19] F. Machefert,[14] F. Maciuc,[43] B. Mack,[69] I. Mackay,[64] L. M. Mackey,[69] L. R. Madhan Mohan,[56] M. J. Madurai,[54] D. Magdalinski,[38] D. Maisuzenko,[44] J. J. Malczewski,[41] S. Malde,[64] L. Malentacca,[49] A. Malinin,[44] T. Maltsev,[44] G. Manca,[32,o] G. Mancinelli,[13] C. Mancuso,[14] R. Manera Escalero,[45] F. M. Manganella,[37] D. Manuzzi,[25] D. Marangotto,[30,l] J. F. Marchand,[10] R. Marchevski,[50] U. Marconi,[25] E. Mariani,[16] S. Mariani,[49] C. Marin Benito,[45] J. Marks,[22] A. M. Marshall,[55] L. Martel,[64] G. Martelli,[34] G. Martellotti,[36] L. Martinazzoli,[49] M. Martinelli,[31,c] D. Martinez Gomez,[81] D. Martinez Santos,[84] F. Martinez Vidal,[48] A. Martorell i Granollers,[46] A. Massafferri,[2] R. Matev,[49] A. Mathad,[49] V. Matiunin,[44] C. Matteuzzi,[69] K. R. Mattioli,[15] A. Mauri,[62] E. Maurice,[15] J. Mauricio,[45] P. Mayencourt,[50] J. Mazorra de Cos,[48] M. Mazurek,[42] M. McCann,[62] T. H. McGrath,[63] N. T. McHugh,[60] A. McNab,[63] R. McNulty,[23] B. Meadows,[66] G. Meier,[19] D. Melnychuk,[42] D. Mendoza Granada,[16] P. Menendez Valdes Perez,[47] F. M. Meng,[4,m] M. Merk,[38,82] A. Merli,[50,30] L. Meyer Garcia,[67] D. Miao,[5,7] H. Miao,[7] M. Mikhasenko,[78] D. A. Milanes,[77,x] A. Minotti,[31,c] E. Minucci,[28] T. Miralles,[11] B. Mitreska,[19] D. S. Mitzel,[19] A. Modak,[58] L. Moeser,[19] R. D. Moise,[17] E. F. Molina Cardenas,[87] T. Mombächer,[49] M. Monk,[57,1] S. Monteil,[11] A. Morcillo Gomez,[47] G. Morello,[28] M. J. Morello,[35,k] M. P. Morgenthaler,[22] A. Moro,[31,c] J. Moron,[40] W. Morren,[38] A. B. Morris,[49] A. G. Morris,[13] R. Mountain,[69] H. Mu,[4,m] Z. M. Mu,[6] E. Muhammad,[57] F. Muheim,[59] M. Mulder,[81] K. Müller,[51] F. Muñoz-Rojas,[9] R. Murta,[62] V. Mytrochenko,[52] P. Naik,[61] T. Nakada,[50] R. Nandakumar,[58] T. Nanut,[49] I. Nasteva,[3] M. Needham,[59] E. Nekrasova,[44] N. Neri,[30,l] S. Neubert,[18] N. Neufeld,[49] P. Neustroev,[44] J. Nicolini,[49] D. Nicotra,[82] E. M. Niel,[15] N. Nikitin,[44] L. Nisi,[19] Q. Niu,[74] P. Nogarolli,[3] P. Nogga,[18] C. Normand,[55] J. Novoa Fernandez,[47] G. Nowak,[66] C. Nunez,[87] H. N. Nur,[60] A. Oblakowska-Mucha,[40]

V. Obraztsov,[44] T. Oeser,[17] A. Okhotnikov,[44] O. Okhrimenko,[53] R. Oldeman,[32,o] F. Oliva,[59,49] E. Olivart Pino,[45] M. Olocco,[19] C. J. G. Onderwater,[82] R. H. O'Neil,[49] J. S. Ordonez Soto,[11] D. Osthues,[19] J. M. Otalora Goicochea,[3] P. Owen,[51] A. Oyanguren,[48] O. Ozcelik,[49] F. Paciolla,[35,y] A. Padee,[42] K. O. Padeken,[18] B. Pagare,[47] T. Pajero,[49] A. Palano,[24] M. Palutan,[28] C. Pan,[75] X. Pan,[4,m] S. Panebianco,[12] G. Panshin,[5] L. Paolucci,[63] A. Papanestis,[58] M. Pappagallo,[24,q] L. L. Pappalardo,[26] C. Pappenheimer,[66] C. Parkes,[63] D. Parmar,[78] B. Passalacqua,[26,g] G. Passaleva,[27] D. Passaro,[35,49,k] A. Pastore,[24] M. Patel,[62] J. Patoc,[64] C. Patrignani,[25,i] A. Paul,[69] C. J. Pawley,[82] A. Pellegrino,[38] J. Peng,[5,7] X. Peng,[74] M. Pepe Altarelli,[28] S. Perazzini,[25] D. Pereima,[44] H. Pereira Da Costa,[68] M. Pereira Martinez,[47] A. Pereiro Castro,[47] C. Perez,[46] P. Perret,[11] A. Perrevoort,[81] A. Perro,[49,13] M. J. Peters,[66] K. Petridis,[55] A. Petrolini,[29,j] S. Pezzulo,[29,j] J. P. Pfaller,[66] H. Pham,[69] L. Pica,[35,k] M. Piccini,[34] L. Piccolo,[32] B. Pietrzyk,[10] G. Pietrzyk,[14] R. N. Pilato,[61] D. Pinci,[36] F. Pisani,[49] M. Pizzichemi,[31,49,c] V. M. Placinta,[43] M. Plo Casasus,[47] T. Poeschl,[49] F. Polci,[16] M. Poli Lener,[28] A. Poluektov,[13] N. Polukhina,[44] I. Polyakov,[63] E. Polycarpo,[3] S. Ponce,[49] D. Popov,[7,49] S. Poslavskii,[44] K. Prasanth,[59] C. Prouve,[84] D. Provenzano,[32,49,o] V. Pugatch,[53] G. Punzi,[35,u] J. R. Pybus,[68] S. Qasim,[51] Q. Q. Qian,[6] W. Qian,[7] N. Qin,[4,m] S. Qu,[4,m] R. Quagliani,[49] R. I. Rabadan Trejo,[57] R. Racz,[80] J. H. Rademacker,[55] M. Rama,[35] M. Ramírez García,[87] V. Ramos De Oliveira,[70] M. Ramos Pernas,[57] M. S. Rangel,[3] F. Ratnikov,[44] G. Raven,[39] M. Rebollo De Miguel,[48] F. Redi,[30,w] J. Reich,[55] F. Reiss,[20] Z. Ren,[7] P. K. Resmi,[64] M. Ribalda Galvez,[45] R. Ribatti,[50] G. Ricart,[15,12] D. Riccardi,[35,k] S. Ricciardi,[58] K. Richardson,[65] M. Richardson-Slipper,[56] K. Rinnert,[61] P. Robbe,[14,49] G. Robertson,[60] E. Rodrigues,[61] A. Rodriguez Alvarez,[45] E. Rodriguez Fernandez,[47] J. A. Rodriguez Lopez,[77] E. Rodriguez Rodriguez,[49] J. Roensch,[19] A. Rogachev,[44] A. Rogovskiy,[58] D. L. Rolf,[19] P. Roloff,[49] V. Romanovskiy,[66] A. Romero Vidal,[47] G. Romolini,[26,49] F. Ronchetti,[50] T. Rong,[6] M. Rotondo,[28] S. R. Roy,[22] M. S. Rudolph,[69] M. Ruiz Diaz,[22] R. A. Ruiz Fernandez,[47] J. Ruiz Vidal,[82] J. J. Saavedra-Arias,[9] J. J. Saborido Silva,[47] S. E. R. Sacha Emile R.,[49] N. Sagidova,[44] D. Sahoo,[79] N. Sahoo,[54] B. Saitta,[32,o] M. Salomoni,[31,49,c] I. Sanderswood,[48] R. Santacesaria,[36] C. Santamarina Rios,[47] M. Santimaria,[28] L. Santoro,[2] E. Santovetti,[37] A. Saputi,[26,49] D. Saranin,[44] A. Sarnatskiy,[81] G. Sarpis,[49] M. Sarpis,[80] C. Satriano,[36,z] M. Saur,[74] D. Savrina,[44] H. Sazak,[17] F. Sborzacchi,[49,28] A. Scarabotto,[19] S. Schael,[17] S. Scherl,[61] M. Schiller,[22] H. Schindler,[49] M. Schmelling,[21] B. Schmidt,[49] N. Schmidt,[68] S. Schmitt,[17] H. Schmitz,[18] O. Schneider,[50] A. Schopper,[62] N. Schulte,[19] M. H. Schune,[14] G. Schwering,[17] B. Sciascia,[28] A. Sciuccati,[49] G. Scriven,[82] I. Segal,[78] S. Sellam,[47] A. Semennikov,[44] T. Senger,[51] M. Senghi Soares,[39] A. Sergi,[29,49,j] N. Serra,[51] L. Sestini,[27] A. Seuthe,[19] B. Sevilla Sanjuan,[46] Y. Shang,[6] D. M. Shangase,[87] M. Shapkin,[44] R. S. Sharma,[69] I. Shchemerov,[44] L. Shchutska,[50] T. Shears,[61] L. Shekhtman,[44] Z. Shen,[38] S. Sheng,[5,7] V. Shevchenko,[44] B. Shi,[7] Q. Shi,[7] W. S. Shi,[73] Y. Shimizu,[14] E. Shmanin,[25] R. Shorkin,[44] J. D. Shupperd,[69] R. Silva Coutinho,[69] G. Simi,[33,s] S. Simone,[24,q] M. Singha,[79] N. Skidmore,[57] T. Skwarnicki,[69] M. W. Slater,[54] E. Smith,[65] K. Smith,[68] M. Smith,[62] L. Soares Lavra,[59] M. D. Sokoloff,[66] F. J. P. Soler,[60] A. Solomin,[55] A. Solovev,[44] K. Solovieva,[20] N. S. Sommerfeld,[18] R. Song,[1] Y. Song,[50] Y. Song,[4,m] Y. S. Song,[6] F. L. Souza De Almeida,[69] B. Souza De Paula,[3] K. M. Sowa,[40] E. Spadaro Norella,[29,j] E. Spedicato,[25] J. G. Speer,[19] P. Spradlin,[60] V. Sriskaran,[49] F. Stagni,[49] M. Stahl,[78] S. Stahl,[49] S. Stanislaus,[64] M. Stefaniak,[88] E. N. Stein,[49] O. Steinkamp,[51] H. Stevens,[19] D. Strekalina,[44] Y. Su,[7] F. Suljik,[64] J. Sun,[32] J. Sun,[63] L. Sun,[75] D. Sundfeld,[2] W. Sutcliffe,[51] V. Svintozelskyi,[48] K. Swientek,[40] F. Swystun,[56] A. Szabelski,[42] T. Szumlak,[40] Y. Tan,[4,m] Y. Tang,[75] Y. T. Tang,[7] M. D. Tat,[22] J. A. Teijeiro Jimenez,[47] A. Terentev,[44] F. Terzuoli,[35,y] F. Teubert,[49] E. Thomas,[49] D. J. D. Thompson,[54] A. R. Thomson-Strong,[59] H. Tilquin,[62] V. Tisserand,[11] S. T'Jampens,[10] M. Tobin,[5] T. T. Todorov,[20] L. Tomassetti,[26,g] G. Tonani,[30] X. Tong,[6] T. Tork,[30] D. Torres Machado,[2] L. Toscano,[19] D. Y. Tou,[4,m] C. Trippl,[46] G. Tuci,[22] N. Tuning,[38] L. H. Uecker,[22] A. Ukleja,[40] D. J. Unverzagt,[22] A. Upadhyay,[49] B. Urbach,[59] A. Usachov,[39] A. Ustyuzhanin,[44] U. Uwer,[22] V. Vagnoni,[25] V. Valcarce Cadenas,[47] G. Valenti,[25] N. Valls Canudas,[49] J. van Eldik,[49] H. Van Hecke,[68] E. van Herwijnen,[62] C. B. Van Hulse,[47,aa] R. Van Laak,[50] M. van Veghel,[38] G. Vasquez,[51] R. Vazquez Gomez,[45] P. Vazquez Regueiro,[47] C. Vázquez Sierra,[84] S. Vecchi,[26] J. Velilla Serna,[48] J. J. Velthuis,[55] M. Veltri,[27,bb] A. Venkateswaran,[50] M. Verdoglia,[32] M. Vesterinen,[57] W. Vetens,[69] D. Vico Benet,[64] P. Vidrier Villalba,[45] M. Vieites Diaz,[47,49] X. Vilasis-Cardona,[46] E. Vilella Figueras,[61] A. Villa,[25] P. Vincent,[16] B. Vivacqua,[3]

F. C. Volle,[54] D. vom Bruch,[13] N. Voropaev,[44] K. Vos,[82] C. Vrahas,[59] J. Wagner,[19] J. Walsh,[35] E. J. Walton,[1,57] G. Wan,[6] A. Wang,[7] B. Wang,[5] C. Wang,[22] G. Wang,[8] H. Wang,[74] J. Wang,[6] J. Wang,[5] J. Wang,[4,m] J. Wang,[75] M. Wang,[49] N. W. Wang,[7] R. Wang,[55] X. Wang,[8] X. Wang,[73] X. W. Wang,[62] Y. Wang,[76] Y. Wang,[6] Y. H. Wang,[74] Z. Wang,[14] Z. Wang,[4,m] Z. Wang,[30] J. A. Ward,[57] M. Waterlaat,[49] N. K. Watson,[54] D. Websdale,[62] Y. Wei,[6] J. Wendel,[84] B. D. C. Westhenry,[55] C. White,[56] M. Whitehead,[60] E. Whiter,[54] A. R. Wiederhold,[63] D. Wiedner,[19] M. A. Wiegertjes,[38] C. Wild,[64] G. Wilkinson,[64,49] M. K. Wilkinson,[66] M. Williams,[65] M. J. Williams,[49] M. R. J. Williams,[59] R. Williams,[56] S. Williams,[55] Z. Williams,[55] F. F. Wilson,[58] M. Winn,[12] W. Wislicki,[42] M. Witek,[41] L. Witola,[19] T. Wolf,[22] E. Wood,[56] G. Wormser,[14] S. A. Wotton,[56] H. Wu,[69] J. Wu,[8] X. Wu,[75] Y. Wu,[6,56] Z. Wu,[7] K. Wyllie,[49] S. Xian,[73] Z. Xiang,[5] Y. Xie,[8] T. X. Xing,[30] A. Xu,[35,k] L. Xu,[4,m] L. Xu,[4,m] M. Xu,[49] Z. Xu,[49] Z. Xu,[7] Z. Xu,[5] K. Yang,[62] X. Yang,[6] Y. Yang,[15] Z. Yang,[6] V. Yeroshenko,[14] H. Yeung,[63] H. Yin,[8] X. Yin,[7] C. Y. Yu,[6] J. Yu,[72] X. Yuan,[5] Y Yuan,[5,7] E. Zaffaroni,[50] J. A. Zamora Saa,[71] M. Zavertyaev,[21] M. Zdybal,[41] F. Zenesini,[25] C. Zeng,[5,7] M. Zeng,[4,m] C. Zhang,[6] D. Zhang,[8] J. Zhang,[7] L. Zhang,[4,m] R. Zhang,[8] S. Zhang,[72] S. Zhang,[64] Y. Zhang,[6] Y. Z. Zhang,[4,m] Z. Zhang,[4,m] Y. Zhao,[22] A. Zhelezov,[22] S. Z. Zheng,[6] X. Z. Zheng,[4,m] Y. Zheng,[7] T. Zhou,[6] X. Zhou,[8] Y. Zhou,[7] V. Zhovkovska,[57] L. Z. Zhu,[7] X. Zhu,[4,m] X. Zhu,[8] Y. Zhu,[17] V. Zhukov,[17] J. Zhuo,[48] Q. Zou,[5,7] D. Zuliani,[33,s] and G. Zunica[28]

(LHCb Collaboration)

[1]*School of Physics and Astronomy, Monash University, Melbourne, Australia*
[2]*Centro Brasileiro de Pesquisas Físicas (CBPF), Rio de Janeiro, Brazil*
[3]*Universidade Federal do Rio de Janeiro (UFRJ), Rio de Janeiro, Brazil*
[4]*Department of Engineering Physics, Tsinghua University, Beijing, China*
[5]*Institute of High Energy Physics (IHEP), Beijing, China*
[6]*School of Physics State Key Laboratory of Nuclear Physics and Technology, Peking University, Beijing, China*
[7]*University of Chinese Academy of Sciences, Beijing, China*
[8]*Institute of Particle Physics, Central China Normal University, Wuhan, Hubei, China*
[9]*Consejo Nacional de Rectores (CONARE), San Jose, Costa Rica*
[10]*Université Savoie Mont Blanc, CNRS, IN2P3-LAPP, Annecy, France*
[11]*Université Clermont Auvergne, CNRS/IN2P3, LPC, Clermont-Ferrand, France*
[12]*Université Paris-Saclay, Centre d'Etudes de Saclay (CEA), IRFU, Saclay, France, Gif-Sur-Yvette, France*
[13]*Aix Marseille Univ, CNRS/IN2P3, CPPM, Marseille, France*
[14]*Université Paris-Saclay, CNRS/IN2P3, IJCLab, Orsay, France*
[15]*Laboratoire Leprince-Ringuet, CNRS/IN2P3, Ecole Polytechnique, Institut Polytechnique de Paris, Palaiseau, France*
[16]*LPNHE, Sorbonne Université, Paris Diderot Sorbonne Paris Cité, CNRS/IN2P3, Paris, France*
[17]*I. Physikalisches Institut, RWTH Aachen University, Aachen, Germany*
[18]*Universität Bonn—Helmholtz-Institut für Strahlen und Kernphysik, Bonn, Germany*
[19]*Fakultät Physik, Technische Universität Dortmund, Dortmund, Germany*
[20]*Physikalisches Institut, Albert-Ludwigs-Universität Freiburg, Freiburg, Germany*
[21]*Max-Planck-Institut für Kernphysik (MPIK), Heidelberg, Germany*
[22]*Physikalisches Institut, Ruprecht-Karls-Universität Heidelberg, Heidelberg, Germany*
[23]*School of Physics, University College Dublin, Dublin, Ireland*
[24]*INFN Sezione di Bari, Bari, Italy*
[25]*INFN Sezione di Bologna, Bologna, Italy*
[26]*INFN Sezione di Ferrara, Ferrara, Italy*
[27]*INFN Sezione di Firenze, Firenze, Italy*
[28]*INFN Laboratori Nazionali di Frascati, Frascati, Italy*
[29]*INFN Sezione di Genova, Genova, Italy*
[30]*INFN Sezione di Milano, Milano, Italy*
[31]*INFN Sezione di Milano-Bicocca, Milano, Italy*
[32]*INFN Sezione di Cagliari, Monserrato, Italy*
[33]*INFN Sezione di Padova, Padova, Italy*
[34]*INFN Sezione di Perugia, Perugia, Italy*
[35]*INFN Sezione di Pisa, Pisa, Italy*
[36]*INFN Sezione di Roma La Sapienza, Roma, Italy*

[37]INFN Sezione di Roma Tor Vergata, Roma, Italy
[38]Nikhef National Institute for Subatomic Physics, Amsterdam, Netherlands
[39]Nikhef National Institute for Subatomic Physics and VU University Amsterdam, Amsterdam, Netherlands
[40]AGH—University of Krakow, Faculty of Physics and Applied Computer Science, Kraków, Poland
[41]Henryk Niewodniczanski Institute of Nuclear Physics Polish Academy of Sciences, Kraków, Poland
[42]National Center for Nuclear Research (NCBJ), Warsaw, Poland
[43]Horia Hulubei National Institute of Physics and Nuclear Engineering, Bucharest-Magurele, Romania
[44]Authors affiliated with an institute formerly covered by a cooperation agreement with CERN
[45]ICCUB, Universitat de Barcelona, Barcelona, Spain
[46]La Salle, Universitat Ramon Llull, Barcelona, Spain
[47]Instituto Galego de Física de Altas Enerxías (IGFAE), Universidade de Santiago de Compostela, Santiago de Compostela, Spain
[48]Instituto de Fisica Corpuscular, Centro Mixto Universidad de Valencia—CSIC, Valencia, Spain
[49]European Organization for Nuclear Research (CERN), Geneva, Switzerland
[50]Institute of Physics, Ecole Polytechnique Fédérale de Lausanne (EPFL), Lausanne, Switzerland
[51]Physik-Institut, Universität Zürich, Zürich, Switzerland
[52]NSC Kharkiv Institute of Physics and Technology (NSC KIPT), Kharkiv, Ukraine
[53]Institute for Nuclear Research of the National Academy of Sciences (KINR), Kyiv, Ukraine
[54]School of Physics and Astronomy, University of Birmingham, Birmingham, United Kingdom
[55]H.H. Wills Physics Laboratory, University of Bristol, Bristol, United Kingdom
[56]Cavendish Laboratory, University of Cambridge, Cambridge, United Kingdom
[57]Department of Physics, University of Warwick, Coventry, United Kingdom
[58]STFC Rutherford Appleton Laboratory, Didcot, United Kingdom
[59]School of Physics and Astronomy, University of Edinburgh, Edinburgh, United Kingdom
[60]School of Physics and Astronomy, University of Glasgow, Glasgow, United Kingdom
[61]Oliver Lodge Laboratory, University of Liverpool, Liverpool, United Kingdom
[62]Imperial College London, London, United Kingdom
[63]Department of Physics and Astronomy, University of Manchester, Manchester, United Kingdom
[64]Department of Physics, University of Oxford, Oxford, United Kingdom
[65]Massachusetts Institute of Technology, Cambridge, Massachusetts, USA
[66]University of Cincinnati, Cincinnati, Ohio, USA
[67]University of Maryland, College Park, Maryland, USA
[68]Los Alamos National Laboratory (LANL), Los Alamos, New Mexico, USA
[69]Syracuse University, Syracuse, New York, USA
[70]Pontifícia Universidade Católica do Rio de Janeiro (PUC-Rio), Rio de Janeiro, Brazil
(associated with Universidade Federal do Rio de Janeiro (UFRJ), Rio de Janeiro, Brazil)
[71]Universidad Andres Bello, Santiago, Chile (associated with Physik-Institut, Universität Zürich, Zürich, Switzerland)
[72]School of Physics and Electronics, Hunan University, Changsha City, China
(associated with Institute of Particle Physics, Central China Normal University, Wuhan, Hubei, China)
[73]Guangdong Provincial Key Laboratory of Nuclear Science, Guangdong-Hong Kong Joint Laboratory of Quantum Matter, Institute of Quantum Matter, South China Normal University, Guangzhou, China
(associated with Department of Engineering Physics, Tsinghua University, Beijing, China)
[74]Lanzhou University, Lanzhou, China (associated with Institute Of High Energy Physics (IHEP), Beijing, China)
[75]School of Physics and Technology, Wuhan University, Wuhan, China
(associated with Department of Engineering Physics, Tsinghua University, Beijing, China)
[76]Henan Normal University, Xinxiang, China (associated with Institute of Particle Physics, Central China Normal University, Wuhan, Hubei, China)
[77]Departamento de Fisica, Universidad Nacional de Colombia, Bogota, Colombia (associated with LPNHE, Sorbonne Université, Paris Diderot Sorbonne Paris Cité, CNRS/IN2P3, Paris, France)
[78]Ruhr Universitaet Bochum, Fakultaet für Physik und Astronomie, Bochum, Germany (associated with Fakultät Physik, Technische Universität Dortmund, Dortmund, Germany)
[79]Eotvos Lorand University, Budapest, Hungary (associated with European Organization for Nuclear Research (CERN), Geneva, Switzerland)
[80]Faculty of Physics, Vilnius University, Vilnius, Lithuania (associated with Physikalisches Institut, Albert-Ludwigs-Universität Freiburg, Freiburg, Germany)
[81]Van Swinderen Institute, University of Groningen, Groningen, Netherlands
(associated with Nikhef National Institute for Subatomic Physics, Amsterdam, Netherlands)
[82]Universiteit Maastricht, Maastricht, Netherlands (associated with Nikhef National Institute for Subatomic Physics, Amsterdam, Netherlands)
[83]Tadeusz Kosciuszko Cracow University of Technology, Cracow, Poland
(associated with Henryk Niewodniczanski Institute of Nuclear Physics Polish Academy of Sciences, Kraków, Poland)

[84]*Universidade da Coruña, A Coruña, Spain (associated with La Salle, Universitat Ramon Llull, Barcelona, Spain)*
[85]*Department of Physics and Astronomy, Uppsala University, Uppsala, Sweden (associated with School of Physics and Astronomy, University of Glasgow, Glasgow, United Kingdom)*
[86]*Taras Schevchenko University of Kyiv, Faculty of Physics, Kyiv, Ukraine (associated with Université Paris-Saclay, CNRS/IN2P3, IJCLab, Orsay, France)*
[87]*University of Michigan, Ann Arbor, Michigan, USA (associated with Syracuse University, Syracuse, New York, USA)*
[88]*Ohio State University, Columbus, Ohio, USA (associated with Los Alamos National Laboratory (LANL), Los Alamos, New Mexico, USA)*

[a]Deceased.
[b]Also at Lamarr Institute for Machine Learning and Artificial Intelligence, Dortmund, Germany.
[c]Also at Università degli Studi di Milano-Bicocca, Milano, Italy.
[d]Also at Università di Roma Tor Vergata, Roma, Italy.
[e]Also at Università di Modena e Reggio Emilia, Modena, Italy.
[f]Also at Department of Physics and Astronomy, University of Victoria, Victoria, British Columbia, Canada.
[g]Also at Università di Ferrara, Ferrara, Italy.
[h]Also at Universidade Estadual de Campinas (UNICAMP), Campinas, Brazil.
[i]Also at Università di Bologna, Bologna, Italy.
[j]Also at Università di Genova, Genova, Italy.
[k]Also at Scuola Normale Superiore, Pisa, Italy.
[l]Also at Università degli Studi di Milano, Milano, Italy.
[m]Also at Center for High Energy Physics, Tsinghua University, Beijing, China.
[n]Also at Universidad Nacional Autónoma de Honduras, Tegucigalpa, Honduras.
[o]Also at Università di Cagliari, Cagliari, Italy.
[p]Also at Centro Federal de Educacão Tecnológica Celso Suckow da Fonseca, Rio De Janeiro, Brazil.
[q]Also at Università di Bari, Bari, Italy.
[r]Also at Università di Perugia, Perugia, Italy.
[s]Also at Università di Padova, Padova, Italy.
[t]Also at LIP6, Sorbonne Université, Paris, France.
[u]Also at Università di Pisa, Pisa, Italy.
[v]Also at Hangzhou Institute for Advanced Study, UCAS, Hangzhou, China.
[w]Also at Università di Bergamo, Bergamo, Italy.
[x]Also at Universidad de Ingeniería y Tecnología (UTEC), Lima, Peru.
[y]Also at Università di Siena, Siena, Italy.
[z]Also at Università della Basilicata, Potenza, Italy.
[aa]Also at Universidad de Alcalá, Alcalá de Henares, Spain.
[bb]Also at Università di Urbino, Urbino, Italy.